MICROSTRUCTURAL EFFECTS IN STRESS CONCENTRATION AND FRACTURE PROBLEMS IN ROCK MECHANICS

J. Sulem, CERMES, Ecole Nationale des Ponts et Chaussées / LCPC, France
I. Vardoulakis, National Technical University of Athens, Greece
G. Exadaktylos, Technical University of Crete, Greece

Abstract:

Failure criteria for rocks usually involve only stresses and are thus suited primarily for homogeneous states of stresses. Since in rock mechanics highly inhomogeneous stresses may occur, it is possible that stress-gradients have some effects of failure mechanism. As mentioned by Mindlin (1963), the apparent strength of rock-type materials is affected by strain gradient. It is observed that brittle failure and the onset of static yielding in the presence of stress concentration occur at higher loads than might be expected on the basis of stress concentration factors calculated from the theory of elasticity. In general, increasing strain gradients appear to make some materials stronger and to a degree that depends upon grain size. In order to capture microstructural effects in stress concentration problems it appears necessary to resort to continuum models with microstructure to describe correctly the deformation process at small scale. These generalized continua usually contain additional kinematical degrees of freedom (Cosserat continuum) and/or higher deformation gradients (higher grade continuum). Rotation gradients and higher velocity gradients introduce a material length scale into the problem, which allow to assess the effect of scale. In this paper some examples of high stress concentration problems as caused by singular stress distribution (indentation and crack problems) are studied and solved analytically within the frame of gradient elasticity with surface energy. The potential of the theory in order to interpret scale effects, i.e. the influence of the size of the loading strip on the response of the material for indentation problems or the dependence of fracture toughness of the material on the size of the crack for crack problems is presented.

1 INTRODUCTION

Failure criteria for rocks usually involve only stresses and are thus suited primarily for homogeneous states of stresses. Since in rock mechanics highly inhomogeneous stresses may occur, it is possible that stress-gradients have some effects of failure mechanism. As mentioned by Mindlin (1963), the apparent strength of rock-type materials is affected by strain gradient. It is observed that brittle failure and the onset of static yielding in the presence of stress concentration occur at higher loads than might be expected on the basis of stress concentration factors calculated from the theory of elasticity. In the framework of continuum theories, quantitites such as stress and strain, represent statistical mean values taken over very small ranges of volume. Consequently continuum theories cannot give satisfying predictions of the behaviour of the material within very small ranges of volume, if high gradients of stress and strain occur. Especially standard continuum-mechanics theories cannot describe situations dominated by microstructural effect, e.g. load or geometrically induced stress singularities, since the influence of these effects is not properly accounted by the standard continuum theories.

Let us for simplicity consider an one-dimensional example and let $y = f(x)$ be a field (e.g.

the density ρ at position x), whose mean value is computed over a small but finite averaging or sampling length L with the point x as its center-point,

$$< y >= \frac{1}{L} \int_{-L/2}^{+L/2} f(x+\xi) d\xi \tag{1}$$

If the field f(x) varies more or less linearly in the considered sampling region, then it is approximated locally by a linear function, using an 1-term Taylor series expansion of the function f around point x,

$$f(x+\xi) \approx f(x) + f'(x)\xi \tag{2}$$

In the trivial case when the field f is indeed constant, then the first and all higher derivatives vanish, and indeed the local value coincides with the average value. However, this is also true in case when the field varies locally linearly. Indeed we may then identify the field with its mean value over the considered averaging length, because, following the 'trapezoidal' rule of integration, the mean value of a linearly varying field in an interval is equal to the value of it in the *midpoint* of the sampling interval,

$$y = < y > \tag{3}$$

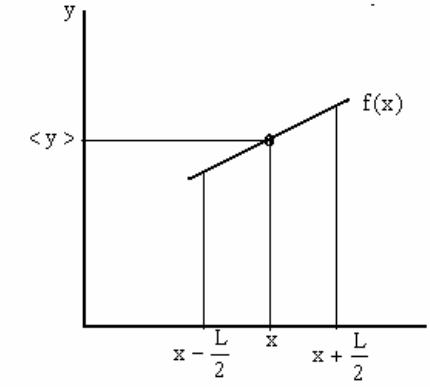

Figure 1: The simple trapezoidal rule of averaging

In this case the 'local' value y and the 'non-local' value <y> coincide. In a field theory where local values are identified with mean values, according to the rule (3), are called simple theories and the corresponding continua, locally homogeneous.
In case however, where the field in the considered sampling interval is not described satisfactorily by a linear function, then of course we have to assume that it possesses some curvature. In this case the above formula (3) must be corrected accordingly, since a linear fit of the data does suffice for the satisfactory description of the field locally. Thus we have to approximate it at least by a 2-term Taylor-series expansion around point x,

$$f(x+\xi) \approx f(x) + f'(x)\xi + \frac{1}{2} f''(x)\xi^2 \tag{4}$$

We notice that in the midpoint integration rule the effect of the first derivative is null. Thus for 'quadratically' varying fields, computational rule (3) must be enhanced, so as to incorporate the effect of curvature,

$$y =< y > -\frac{1}{24} L^2 \left(\frac{d^2 y}{dx^2} \right)_x \tag{5}$$

Field theories, which are based on averaging rules that include the effect of higher gradients, are called *higher gradient theories*. In particular above rule (5) represents a 2nd gradient rule, and can be readily generalized in 2 and 3 dimensions by introducing the Laplacian operator instead of the second derivative. Such higher gradient theories can be formalised within the frame of generalised continuum theories. These theories were rediscovered and reopened in various special forms and degree of complexity in the sixties. The state of the art of this evolution in the mid-sixties was refected in a collection of papers presented at the historical IUTAM Symposium on the "Mechanics of Generalised Continua" (Kröner 1967). Newly the interest to such theories is rekindled through the idea of connecting micromechanics with fracture and failure of solids (see for example extensive literature review in Vardoulakis and Sulem 1995)

These generalised continua usually contain additional kinematical degrees of freedom (Cosserat continuum) and/or higher deformation gradients (higher grade continuum). Rotation gradients and higher velocity gradients introduce a material length scale into the problem, which allow to assess the effect of scale. In this paper some examples of high stress concentration problems as caused by singular stress distribution (indentation and crack problems) are studied and solved analytically within the frame of gradient elasticity with surface energy. The potential of the theory in order to interpret scale effects, i.e. the influence of the size of the loading strip on the response of the material for indentation problems or the dependence of fracture toughness of the material on the size of the crack for crack problems is presented.

2 MINDLIN'S FORMALISM OF MICROSTRUCTURE

The description of statics and kinematics of continuous media with microstructure has been studied in a systematic way by Germain (1973a,b) through the application of the virtual work principle and following the formalism introduced by Mindlin (1964).

2.1 Kinematics

In a classical description, a continuum is a continuous distribution of particles, each of them being represented geometrically by a point X and characterised kinematically by a velocity v. In a theory which takes into account the microstructure of the material, each particle is viewed as a continuum C(X) of small extent around the point X.

Consider a body B which at a configuration C(t) occupies the volume V with boundary ∂V. Let x_i and $\bar{x}_i$ (i=1,2,3) be the coordinates of a macro-material particle X in C(t) and $\bar{C} = C(t + \Delta t)$, respectively, measured from a fixed-in-space Cartesian coordinate system. The components of the (infinitesimal) displacement vector of the macro-particle X are defined as

$$\Delta u_i = \bar{x}_i - x_i \tag{6}$$

The infinitesimal macro-strain and macro-rotation are defined as usual as the symmetric and antisymmetric part of the displacement gradient

$$\Delta\varepsilon_{ij} = \frac{1}{2}(\partial_i \Delta u_j + \partial_j \Delta u_i)$$
$$\Delta\omega_{ij} = \frac{1}{2}(\partial_i \Delta u_j - \partial_j \Delta u_i) \tag{7}$$

We assume now that the macro-particle possesses a simple micro-structure defined as follows: In each macro-material particle X we assume that there is a micro-volume V' embedded, in which the spatial position vectors of micro-material particle X' are x'_i and $\bar{x}_i$ in C and $\bar{C}$, respectively. We assume that the position of the micro-particle is measured with respect to a single Cartesian coordinates system (x'_i), parallel to the x_i-system, such that the origin of the coordinates x'_i moves with the macroscopic displacement Δu_i. A micro-displacement $\Delta u_i'$ is defined, with components

$$\Delta u_i' = \bar{x}_i' - x_i' \tag{8}$$

A *micromorphic continuum of order 1* is obtained if the micro-displacement Δu_i is expressed as a first order Taylor expansion of the coordinates x'_i of X', that is

$$\Delta u'_j = x'_i \, \Delta\psi_{ij} \tag{9}$$

Accordingly the quantity

$$\Delta\psi_{ij} = \partial_i \Delta u_j' \tag{10}$$

is called the micro-deformation which we assume to be *homogeneous* in the micro-volume V'. The symmetric part

$$\Delta\psi_{(ij)} = \frac{1}{2}(\partial_i \Delta\psi_j + \partial_j \Delta\psi_i) \tag{11}$$

is called the micro-strain, and the antisymmetric part

$$\Delta\psi_{[ij]} = \frac{1}{2}(\partial_i \Delta\psi_j - \partial_j \Delta\psi_i) \tag{12}$$

is called the micro-rotation.
The difference between the macro-displacement gradient and the micro-deformation gradient is called the relative deformation

$$\Delta\gamma_{ij} = \partial_j \Delta u_i - \Delta\psi_{ij} \tag{13}$$

Finally the quantity

$$\Delta\kappa_{ijk} = \partial_i \Delta\psi_{jk} \tag{14}$$

is called the micro-deformation gradient.
The basic kinematic quantities Δu_i and $\Delta\psi_{ij}$ are assumed to be single-valued functions of x_i, leading to the following compatibility conditions

$$\begin{aligned} &e_{mik} e_{nlj} \partial_i \partial_j \Delta\varepsilon_{kl} = 0 \\ &e_{mij} \partial_i \Delta\kappa_{jkl} = 0 \\ &\partial_i (\Delta\varepsilon_{jk} + \Delta\omega_{jk} - \Delta\gamma_{jk}) = \Delta\kappa_{ijk} \end{aligned} \tag{15}$$

where e_{ijk} is the Levy-Civita permutation tensor; i.e. the complete 3rd order antisymmetric tensor

$$\begin{aligned} &\text{if } (i,j,k) = \text{cyclic}(1,2,3) \text{ then } e_{ijk} = 1 \\ &\text{if } (i,j,k) = \text{cyclic}(2,1,3) \text{ then } e_{ijk} = -1 \\ &\qquad\qquad\qquad \text{else } e_{ijk} = 0 \end{aligned} \tag{16}$$

2.2 The principle of virtual work

Germain (1972a,b) suggested a general framework for the foundation of consistent higher grade continuum theories on the basis of the virtual work principle. This approach starts with the definition of the virtual work $\delta w^{(i)}$ of the internal forces at any point, which for a Mindlin-type continuum is defined as follows

$$\delta w^{(i)} = \tau_{ij} \delta\varepsilon_{ij} + \alpha_{ij} \gamma_{ij} + \mu_{ijk} \delta\kappa_{ijk} \tag{17}$$

The expression for the virtual work gives rise to the identification of the corresponding stress tensors. Here, according to (17), the stress tensor, τ_{ij}, which is dual in energy to the macroscopic strain, is symmetric and is called by Mindlin the Cauchy stress. The stress tensor, α_{ij}, which is dual in energy to the relative deformation is called the relative stress, and the higher order stress tensor μ_{ijk}, which is dual in energy to the micro-deformation gradient is called the double stress. By using equation (7) and (15), the work of internal forces become

$$\delta w^{(i)} = \sigma_{ij} \partial_i \delta u_j - \alpha_{ij} \delta\psi_{ij} + \mu_{ijk} \delta\kappa_{ijk} \tag{18}$$

where

$$\sigma_{ij} = \tau_{ij} + \alpha_{ij} \tag{19}$$

is called the total stress tensor.
The definition (17) of the virtual work of internal forces gives rise also to the definition of the virtual work of corresponding external forces, i.e. body forces and surface tractions,

$$\delta W^{(e)} = \int_V f_i \delta u_i dV + \int_{\partial V} t_i \delta u_i dS + \int_V \Phi_{ij} \delta\psi_i dV + \int_{\partial V} T_{ij} \delta\psi_{ij} dS \tag{20}$$

where f_i is identified as the body force per unit volume, t_i as the surface traction per unit surface area. Φ_{ij} is the double-force per unit volume , and T_{ij} is the double-traction per unit surface area.
Using d'Alembert's principle, macro- and micro-inertial terms may be included in the above expression for the virtual work of external forces. In this case in equation (20) the body force f_i may be replaced by $(f_i - \rho\partial_{tt}\Delta u_i)$ and the double body force Φ_{ij} by $(\Phi_{ij} - I_{ijkl}\partial_{tt}\Delta\psi_{kl})$ where I_{ijkl} is an appropriate micro-inertial tensor.
The variations δu_i and $\delta\psi_{ij}$ are treated as independent. Then from the equation of virtual work

$$\int_V \delta w^{(i)} dV = \delta W^{(e)} \tag{21}$$

one obtains two integral equations: one concerning the macro-mechanics of the medium

$$\int_V \left(\sigma_{ij}\partial_i \delta u_j - f_i \delta u_i\right) dV = \int_{\partial V} t_i \delta u_i dS \tag{22}$$

and, an other concerning the micro-mechanics

$$\int_V \left(-\alpha_{ij}\delta\psi_{ij} + \mu_{ijk}\partial_i \delta\psi_{jk} - \Phi_{ij}\delta\psi_{ij}\right) dV = \int_{\partial V} T_{ij}\delta\psi_{ij} dS \tag{23}$$

In order to evaluate these integral equations, the boundary ∂V is divided into complementary parts $\{\partial V_u , \partial V_\sigma\}$ and $\{\partial V_\psi , \partial V_\gamma\}$, respectively, such that

$$\begin{aligned} &\text{on } \partial V_u : \Delta u_i = \delta_i \text{ and } \delta u_i = 0 \\ &\text{on } \partial V_\psi : \Delta\psi_{ij} = \Theta_i \text{ and } \delta\psi_{ij} = 0 \end{aligned} \tag{24}$$

are prescribed. From equations (22) and (24), Gauss' theorem and d'Alembert's principle one obtains the following dynamic equations, holding for the macro- and micro-medium respectively:

$$\text{in V:} \quad \partial_i \sigma_{ij} + f_j = \rho\partial_{tt}\Delta u_j \tag{25}$$

$$\text{on } \partial V_\sigma: \quad n_i \sigma_{ij} = t_j \tag{26}$$

and

$$\text{in V:} \quad \alpha_{jk} + \partial_i \mu_{ijk} + \Phi_{jk} = I_{jkmn}\partial_{tt}\Delta\psi_{mn} \tag{27}$$

$$\text{on } \partial V_\mu: \quad n_i \mu_{ijk} = T_{jk} \tag{28}$$

Notice that according to equation (25) the total stress tensor $\sigma_{ij} = \tau_{ij} + \alpha_{ij}$, is identified with the common (macroscopic) equilibrium stress tensor.

2.3 Micromorphic continuum of order 1

2.3.1 Cosserat continuum

From the Mindlin's formulation of microstructure we can derive the basic equations of a Cosserat continuum and a second-gradient theory. A Cosserat continuum which is a micropolar medium is obtained by assuming that the micro-volume V' moves as a rigid body. Accordingly a Cosserat model is a continuum model that allows both particle displacement and rotation. Consequently, the micro-deformation tensor is purely antisymmetric and is identified with the individual particle rotation $\Delta\omega^c$

$$\begin{aligned} \Delta\psi_{ij} &= \Delta\psi_{[ij]} = \Delta\omega^c_{ij} \\ \Delta\gamma_{ij} &= \Delta\varepsilon_{ij} + (\Delta\omega_{ij} - \Delta\omega^c_{ij}) \end{aligned} \tag{29}$$

and the micro-rotation gradient is identified to the curvature which is also antisymmetric

$$\Delta\kappa_{ijk} = \partial_i \omega^c_{jk} \tag{30}$$

From the above equations we observe that for a Cosserat continuum the symmetric part of the relative deformation $\Delta\gamma_{ij}$ coincides with the macro-strain and that the difference between macro- and micro-deformation appears only in the antisymmetric part of the relative deformation, namely that the individual rotation of a particle does not coincide with the spin of the domain around the particle represented by the macro-rotation $\Delta\omega$.
From the principle of virtual work we can specify the statical quantities involved in a Cosserat continuum. It appears from equation (18) that the relative stress α_{ij} is nothing else but the antisymmetric part of the total stress tensor σ_{ij}. On the other hand, from equation (20) Φ_{ij} and T_{ij} may be assumed, without loss of generality, antisymmetric with respect to i and j.: they define the volumic couple distribution and surface couple stress respectively.
It is obviously easy to get a more classical description when one introduces the adjoints tensors with respect to the indices i and j:

$$\omega^c_{ij} = -e_{ijk}\omega^c_k, \quad \mu_{ijk} = -e_{ijl}m_{kl}, \quad \Phi_{ij} = -e_{ijk}\Phi_k, \quad T_{ij} = -e_{ijk}M_k \tag{31}$$

The interpretation is quite easy: ω^c is a rotation vector interpreted as the individual particle rotation or Cosserat rotation vector, M and Φ are couple densities, m is the couple density stress. Equations (27) and (28) can then be written as

$$\text{in V:} \quad e_{ijk}\sigma_{jk} + \partial_j m_{ij} + \Phi_i = I\partial_{tt}\Delta\omega^c_i \tag{32}$$

$$\text{on } \partial V_\mu: \quad n_i m_{ij} = M_i \tag{33}$$

2.3.2 Second gradient theory

The second gradient theory may be obtained very easily from the theory of micromorphic media of order 1 when one assumes that the particle is subject to the same deformation as the general continuum, i.e.

$$\Delta\psi_{ij} = \partial_i \Delta u_j \tag{34}$$

and consequently in that case relative deformation is vanishing

$$\Delta\gamma_{ij} \equiv 0 \tag{35}$$

The corresponding medium may be called a restricted Mindlin continuum. In the present case u_i and ψ_{ij} are not independent fields and the virtual work equations must be modified accordingly. The micro- and macro-strain tensors are identical and the micro-deformation gradient is the second gradient of the displacement.

3 2ND-GRADIENT ANISOTROPIC ELASTICITY MODEL

3.1 Constitutive equations

The 2nd-gradient elasticity model considered here is based on an original idea of Casal (1961) who introduced in the global strain-energy of a one-dimensional tension bar both a 'volumetric energy' term which includes the contribution of strain gradient and a 'surface energy' term. The one-dimensional Casal's model was generalised into a three dimensional anisotropic gradient-dependent elasticity (Vardoulakis and Sulem 1995) where the following expression for the strain energy function is considered (see also Vardoulakis and Exadaktylos 1999),

$$w = \frac{1}{2}\left(\lambda\varepsilon_{ii}\varepsilon_{jj} + 2G\varepsilon_{ij}\varepsilon_{ji} + \lambda\ell^2\partial_k\varepsilon_{ii}\partial_k\varepsilon_{jj} + 2G\ell^2\partial_k\varepsilon_{ij}\partial_k\varepsilon_{ji} + \lambda\ell_k\partial_k\left(\varepsilon_{ii}\varepsilon_{jj}\right) + G\ell_k\partial_k\left(\varepsilon_{ij}\varepsilon_{ji}\right)\right) \tag{36}$$

where λ and G are the Lamé's constants, ℓ is a characteristic length of the material responsible for volumetric strain-gradient terms and

$$\ell_k = \ell'\nu_k, \quad \nu_k\nu_k = 1 \tag{37}$$

is a material director, ℓ' being another material length responsible for surface strain-gradient terms. Indeed the last two terms in equation (37) have the meaning of a surface energy, since by using the divergence theorem

$$\int_V \ell_k\left(\lambda\partial_k\left(\varepsilon_{ii}\varepsilon_{jj}\right) + 2G\partial_k\left(\varepsilon_{ij}\varepsilon_{ji}\right)\right)dV = \ell'\int_S\left(\lambda\varepsilon_{ii}\varepsilon_{jj} + 2G\varepsilon_{ij}\varepsilon_{ji}\right)\left(\nu_k n_k\right)dS \tag{38}$$

Accordingly, in Casal's model, two material constants with dimension of length ℓ and ℓ' are introduced to characterise the internal and surface capillarity with the following condition for positiveness of the elastic strain energy density

$$-1 < \frac{\ell'}{\ell} < 1 \tag{39}$$

This means in particular that if surface energy terms are included then volume strain-gradient must be also included. It is worth noticing that in Griffith's theory of cracks only surface energy is considered, which is of course inadmissible in the sense of inequality (34). Notice that such a model is by essence anisotropic as it includes the effect of surface tension. Positive values for ℓ' correspond to strengthening due to surface tension whereas negative values correspond to weakening due to material decohesion.

With the above expression for the strain energy function (equation 2) and following Mindlin's (1964) formalism for materials with microstructure, the following constitutive equations are obtained for the total, Cauchy and double stress tensors

$$\begin{aligned}
\sigma_{ij} &= \lambda\delta_{ij}\varepsilon_{kk} + 2G\varepsilon_{ij} - \ell^2\nabla^2\left(\lambda\delta_{ij}\varepsilon_{kk} + 2G\varepsilon_{ij}\right) \\
\tau_{ij} &= \lambda\delta_{ij}\varepsilon_{kk} + 2G\varepsilon_{ij} + \ell_k\partial_k\left(\lambda\delta_{ij}\varepsilon_{kk} + 2G\varepsilon_{ij}\right) \\
\mu_{kij} &= \ell_k\left(\lambda\delta_{ij}\varepsilon_{ll} + 2G\varepsilon_{ij}\right) + \ell^2\partial_k\left(\lambda\delta_{ij}\varepsilon_{ll} + 2G\varepsilon_{ij}\right)
\end{aligned} \tag{40}$$

where δ_{ij} is Kronecker delta. The 27 components μ_{kij} have the character of double forces per unit area. The first subscript of a double stress μ_{kij} designates the normal to the surface across which the component acts; the second and third subscripts have the same significance as the two subscripts of σ_{ij}.

3.2 Plane strain problem

In a Cartesian coordinate system (x,y,z) for the case of plane strain parallel to the xy-plane with

$$\mathbf{u} = \left(u(x,y), v(x,y), 0\right) \tag{41}$$

The components of the strain tensor in plane strain are given by

$$\varepsilon_{xx} = \partial_x u, \quad \varepsilon_{yy} = \partial_y v, \quad \varepsilon_{xy} = \varepsilon_{yx} = \frac{1}{2}\left(\partial_y u + \partial_x v\right), \quad \varepsilon_{zz} = \varepsilon_{xz} = \varepsilon_{yz} = 0 \tag{42}$$

The components of the stress tensor are give by the constitutive equations (40)

$$\begin{aligned}
\sigma_{xx} &= (\lambda + 2G)\partial_x u + \lambda\partial_y v - \ell^2\nabla^2\left[(\lambda + 2G)\partial_x u + \lambda\partial_y v\right] \\
\sigma_{yy} &= (\lambda + 2G)\partial_y v + \lambda\partial_x u - \ell^2\nabla^2\left[(\lambda + 2G)\partial_y v + \lambda\partial_x u\right] \\
\sigma_{xy} &= \sigma_{yx} = G\left(\partial_y u + \partial_x v\right) - \ell^2\nabla^2\left[G\left(\partial_y u + \partial_x v\right)\right] \\
\sigma_{zz} &= \lambda\left(\partial_x u + \partial_y v\right) - \ell^2\nabla^2\left[\lambda\left(\partial_x u + \partial_y v\right)\right] \\
\sigma_{zx} &= \sigma_{zy} = 0
\end{aligned} \tag{43}$$

The only non-vanishing components of the double stress tensor for the half-plane $y \geq 0$ are (equation 40)

$$
\begin{aligned}
\mu_{xxx} &= \ell^2\partial_x\left[(\lambda+2G)\varepsilon_{xx}+\lambda\varepsilon_{yy}\right]\\
\mu_{yxx} &= -\ell'\left[(\lambda+2G)\varepsilon_{xx}+\lambda\varepsilon_{yy}\right]+\ell^2\partial_y\left[(\lambda+2G)\varepsilon_{xx}+\lambda\varepsilon_{yy}\right]\\
\mu_{xyy} &= \ell^2\partial_x\left[(\lambda+2G)\varepsilon_{yy}+\lambda\varepsilon_{xx}\right]\\
\mu_{yyy} &= -\ell'\left[(\lambda+2G)\varepsilon_{yy}+\lambda\varepsilon_{xx}\right]+\ell^2\partial_y\left[(\lambda+2G)\varepsilon_{yy}+\lambda\varepsilon_{xx}\right]\\
\mu_{xxy} &= \mu_{xyx} = 2G\ell^2\partial_x\varepsilon_{xy}, \quad \mu_{yyx} = \mu_{xyx} = -2G\ell'\varepsilon_{xy}+2G\partial_y\varepsilon_{xy}
\end{aligned}
\tag{44}
$$

In the absence of body forces the equilibrium equation (25) becomes

$$\partial_i\sigma_{ij} = 0 \tag{45}$$

3.3 The semi-infinite elastic medium

Plane problems for the half-space $y \geq 0$ are commonly solved using the Fourier transform (Sneddon 1951). We use the "bar notation" to denote 1-D Fourier transform with respect to x:

$$\bar{u}(\xi,y) = \frac{1}{\sqrt{2\pi}}\int_{-\infty}^{+\infty} u(x,y)e^{i\xi x}dx, \quad \bar{v}(\xi,y) = \frac{1}{\sqrt{2\pi}}\int_{-\infty}^{+\infty} v(x,y)e^{i\xi x}dx \tag{46}$$

Accordingly the stress-displacement relations (43) are transformed as

$$
\begin{aligned}
\bar{\sigma}_{xx} &= -(i\xi)(\lambda+2G)\left[(1+\ell^2\xi^2)-\ell^2D^2\right]\bar{u}+\lambda\left[(1+\ell^2\xi^2)D-\ell^2D^3\right]\bar{v}\\
\bar{\sigma}_{yy} &= -(i\xi)\lambda\left[(1+\ell^2\xi^2)-\ell^2D^2\right]\bar{u}+(\lambda+2G)\left[(1+\ell^2\xi^2)D-\ell^2D^3\right]\bar{v}\\
\bar{\sigma}_{xy} &= G\left[(1+\ell^2\xi^2)D-\ell^2D^3\right]\bar{u}-(i\xi)\left[(1+\ell^2\xi^2)-\ell^2D^2\right]\bar{v}
\end{aligned}
\tag{47}
$$

where D≡d/dy and the equilibrium equations as

$$
\begin{aligned}
-i\xi\bar{\sigma}_{xx}+D\bar{\sigma}_{xy} &= 0\\
-i\xi\bar{\sigma}_{xy}+D\bar{\sigma}_{yy} &= 0
\end{aligned}
\tag{48}
$$

leading to the following system of ordinary differential equations

$$
\begin{aligned}
\left[\ell^2D^2-(1+\ell^2\xi^2)\right]\left\{\left[GD^2-(\lambda+2G)\xi^2\right]\bar{u}-i\xi(\lambda+G)D\bar{v}\right\} &= 0\\
\left[\ell^2D^2-(1+\ell^2\xi^2)\right]\left\{\left[(\lambda+2G)D^2-G\xi^2\right]\bar{v}-i\xi(\lambda+G)D\bar{u}\right\} &= 0
\end{aligned}
\tag{49}
$$

On eliminating $\bar{u}$ and $\bar{v}$ from equation (49) we have

$$
\begin{aligned}
(D^2-\xi^2)\left(\ell^2D^2-\left[1+\ell^2\xi^2\right]\right)\bar{u} &= 0\\
(D^2-\xi^2)\left(\ell^2D^2-\left[1+\ell^2\xi^2\right]\right)\bar{v} &= 0
\end{aligned}
\tag{50}
$$

For the case where the gradients effects are negligible, that is $\ell \to 0$, the above equations reduce to those of classical elasticity

$$\begin{aligned}\left(D^2-\xi^2\right)\overline{u}&=0\\ \left(D^2-\xi^2\right)\overline{v}&=0\end{aligned} \tag{51}$$

The general solution of (50) for the half plane $y \geq 0$, considering that the displacements must remain finite for $y \to \infty$ is

$$\begin{aligned}\overline{u}(\xi,y)&=\left[A_1(\xi)+yB_1(\xi)\right]e^{-y|\xi|}+C_1(\xi)e^{-ya(\xi)}\\ \overline{v}(\xi,y)&=\left[A_2(\xi)+yB_2(\xi)\right]e^{-y|\xi|}+C_2(\xi)e^{-ya(\xi)}\end{aligned} \tag{52}$$

where

$$a(\xi)=\sqrt{\xi^2+\frac{1}{\ell^2}} \tag{53}$$

and $A_i(\xi)$, $B_i(\xi)$, $C_i(\xi)$, $(i = 1,2)$ are unknown complex functions to be determined from the boundary conditions of the problem. The components of the stress and double stress tensors in the transform domain can be expressed in terms of the above unknown functions:

$$\begin{aligned}\frac{1}{G}\overline{\sigma}_{xx}(\xi,y)&=\Big\{(-i\xi)(m+2)\left[A_1(\xi)+\left(y+2\ell^2|\xi|\right)B_1(\xi)\right]\\ &\quad+m\left[-|\xi|A_2(\xi)+\left(1-y|\xi|-2\ell^2\xi^2\right)B_2(\xi)\right]\Big\}e^{-y|\xi|}\\ \frac{1}{G}\overline{\sigma}_{yy}(\xi,y)&=\Big\{(-i\xi)m\left[A_1(\xi)+\left(y+2\ell^2|\xi|\right)B_1(\xi)\right]\\ &\quad+(m+2)\left[-|\xi|A_2(\xi)+\left(1-y|\xi|-2\ell^2\xi^2\right)B_2(\xi)\right]\Big\}e^{-y|\xi|}\\ \frac{1}{G}\overline{\sigma}_{xy}(\xi,y)&=\Big\{\left[-|\xi|A_1(\xi)+\left(1-y|\xi|-2\ell^2\xi^2\right)B_1(\xi)\right]\\ &\quad-(i\xi)\left[A_2(\xi)+\left(y+2\ell^2|\xi|\right)B_2(\xi)\right]\Big\}e^{-y|\xi|}\end{aligned} \tag{54}$$

and only the following double stress components

$$\frac{1}{G}\overline{\mu}_{yyy}(\xi,y)=m(i\xi)\left\{\left[\left(\ell'+\ell^2|\xi|\right)A_1(\xi)+\left(\ell' y+\left(\ell^2|\xi|y-1\right)\right)B_1(\xi)\right]e^{-y|\xi|}\right.$$
$$\left.+\left[\ell'+\ell^2\sqrt{\xi^2+\frac{1}{\ell^2}}\right]C_1(\xi)e^{-y\sqrt{\xi^2+\frac{1}{\ell^2}}}\right\}$$
$$+(m+2)\left\{\left[\left(\ell'|\xi|+\ell^2\xi^2\right)A_2(\xi)+\left(-\ell'(1-y|\xi|)+\left(\ell^2 y-2|\xi|\right)\right)B_2(\xi)\right]e^{-y|\xi|}\right.$$
$$\left.+\sqrt{\xi^2+\frac{1}{\ell^2}}\left[\ell'+\ell^2\sqrt{\xi^2+\frac{1}{\ell^2}}\right]C_2(\xi)e^{-y\sqrt{\xi^2+\frac{1}{\ell^2}}}\right\}$$

$$\frac{1}{G}\overline{\mu}_{yyx}(\xi,y)=\left[\left(\ell'+\ell^2|\xi|\right)|\xi|A_1(\xi)+\left(-\ell'\left(1-\ell^2|\xi|y\right)+\ell^2\left(\xi^2 y-2|\xi|\right)\right)B_1(\xi)\right]e^{-y|\xi|}$$
$$\left.+\sqrt{\xi^2+\frac{1}{\ell^2}}\left[\ell'+\ell^2\sqrt{\xi^2+\frac{1}{\ell^2}}\right]C_1(\xi)e^{-y\sqrt{\xi^2+\frac{1}{\ell^2}}}\right\}$$
$$+(i\xi)\left\{\left[\left(\ell'+\ell^2|\xi|\right)A_2(\xi)+\left(\ell' y-\ell^2(1-|\xi|y)\right)B_2(\xi)\right]e^{-y|\xi|}\right.$$
$$\left.+\left[\ell'+\ell^2\sqrt{\xi^2+\frac{1}{\ell^2}}\right]C_2(\xi)e^{-y\sqrt{\xi^2+\frac{1}{\ell^2}}}\right\} \tag{55}$$

where

$$m=\lambda/G=2\nu/(1-2\nu) \tag{56}$$

4 THE INDENTATION PROBLEM

4.1 Classical boundary conditions

The simplest model to represent the effect of an indentor acting at the surface of a material is to consider a half-space with uniform surface pressure over a strip of dimension $2a$. It is assumed that the medium is bounded by a plane. The y axis is taken normal to this plane to point into the medium. Then the boundary conditions are

$$\text{on } y=0 \quad \sigma_{yy}=p(x), \quad \sigma_{xy}=0, \quad \mu_{yyy}=0, \quad \mu_{yyx}=0 \tag{57}$$

with

$$p(x)=\begin{cases}-p_0 & \text{if } |x|\le a\\ 0 & \text{if } |x|>a\end{cases} \tag{58}$$

These boundary conditions can be expressed in the transform domain as

$$\text{on } y=0 \quad \overline{\sigma}_{yy}=\overline{p}(\xi), \quad \overline{\sigma}_{xy}=0, \quad \overline{\mu}_{yyy}=0, \quad \overline{\mu}_{yyx}=0 \tag{59}$$

with

$$\bar{p}(\xi)=\frac{\sin(a\xi)}{\xi} \tag{60}$$

From above boundary conditions (59) and the expressions (54) and (55) for the stress and double stress components, the integration functions $A_i(\xi)$, $B_i(\xi)$, $C_i(\xi)$, (i = 1,2) are determined

$$\begin{aligned}
A_1(\xi)&=-i\frac{\bar{p}(\xi)}{G\xi}\left(\frac{1}{2}-\nu+\ell^2\xi^2\right)\\
A_2(\xi)&=\frac{\bar{p}(\xi)}{G\xi}\left(1-\nu-\ell^2\xi^2\right)\\
B_1(\xi)&=\frac{1}{2G}i\,\mathrm{sgn}(\xi)\bar{p}(\xi)\\
B_2(\xi)&=\frac{1}{2G}\bar{p}(\xi)
\end{aligned} \tag{61}$$

and

$$\begin{aligned}
C_2(\xi)=\frac{-1}{2G}&\frac{\bar{p}(\xi)\ell}{\left(\eta+\sqrt{1+\xi^2\ell^2}\right)\left(1-\nu+\xi^2\ell^2\right)}\Big\{-2\nu\ell^2\xi^2\left(1+2\eta\ell|\xi|+2\ell^2\xi^2\right)\\
&(1-2\nu)\sqrt{1+\xi^2\ell^2}\left[\eta\left(1-2\ell^2\xi^2\right)-2\ell^3|\xi|^3\right]\Big\}
\end{aligned} \tag{62}$$

$$C_1(\xi)=i\frac{(1-\nu)}{\nu}\frac{\sqrt{1+\xi^2\ell^2}}{\ell\xi}C_2(\xi)-\frac{i}{2G}\frac{\bar{p}(\xi)}{\left(\eta+\sqrt{1+\xi^2\ell^2}\right)}\frac{1-2\nu}{\nu\xi}\left\{\eta\left(-1+2\ell^2\xi^2\right)+2\ell^3|\xi|^3\right\}$$

with

$$\eta=\frac{\ell'}{\ell} \tag{63}$$

Substituting the expressions of the functions $A_i(\xi)$, $B_i(\xi)$ (i = 1,2) (equation 56) in equation (54), we obtain the following components of the stress tensor

$$\begin{aligned}
\sigma_{xx}&=-\frac{1}{2\pi}\int_{-\infty}^{\infty}\bar{p}(\xi)\left(1-|\xi|y\right)e^{-|\xi|y-i\xi x}d\xi\\
\sigma_{yy}&=-\frac{1}{2\pi}\int_{-\infty}^{\infty}\bar{p}(\xi)\left(1+|\xi|y\right)e^{-|\xi|y-i\xi x}d\xi\\
\sigma_{xy}&=-\frac{i}{2\pi}\int_{-\infty}^{\infty}y\xi\bar{p}(\xi)e^{-|\xi|y-i\xi x}d\xi
\end{aligned} \tag{64}$$

This expression is similar to the one obtained in classical elasticity (Sneddon 1951). For a uniform pressure acting on the boundary (equation 53) we obtain

$$\sigma_{xx} = -\frac{2}{\pi} p_0 \int_0^{\infty} \frac{1-\xi y}{\xi} e^{-\xi y} \sin(\xi a)\cos(\xi x) d\xi$$
$$\sigma_{yy} = -\frac{2}{\pi} p_0 \int_0^{\infty} \frac{1+\xi y}{\xi} e^{-\xi y} \sin(\xi a)\cos(\xi x) d\xi \quad (65)$$
$$\sigma_{xy} = -\frac{2}{\pi} p_0 y \int_0^{\infty} e^{-\xi y} \sin(\xi a)\sin(\xi x) d\xi$$

The vertical displacement under the indentor has then the following expression

$$v(x,0) = \frac{1}{\sqrt{2\pi}} \int_{-\infty}^{+\infty} \left(A_2(\xi) + C_2(\xi)\right) e^{-i\xi x} d\xi = \sqrt{\frac{2}{\pi}} \int_0^{\infty} \left(A_2(\xi) + C_2(\xi)\right) \cos(\xi x) d\xi \quad (66)$$

In order to demonstrate the effect of higher order gradient terms in the constitutive equations for assessment of scale effect, the ratio between the present gradient solution and the classical one (e.g. Johnson 1985) for the displacement under the indentor ($x = y = 0$) is plotted on Figure 2 for various values of the ratio ℓ'/ℓ and compared to the solution obtained in case of a Cosserat elastic half-space (Sulem and Vardoulakis 1998).

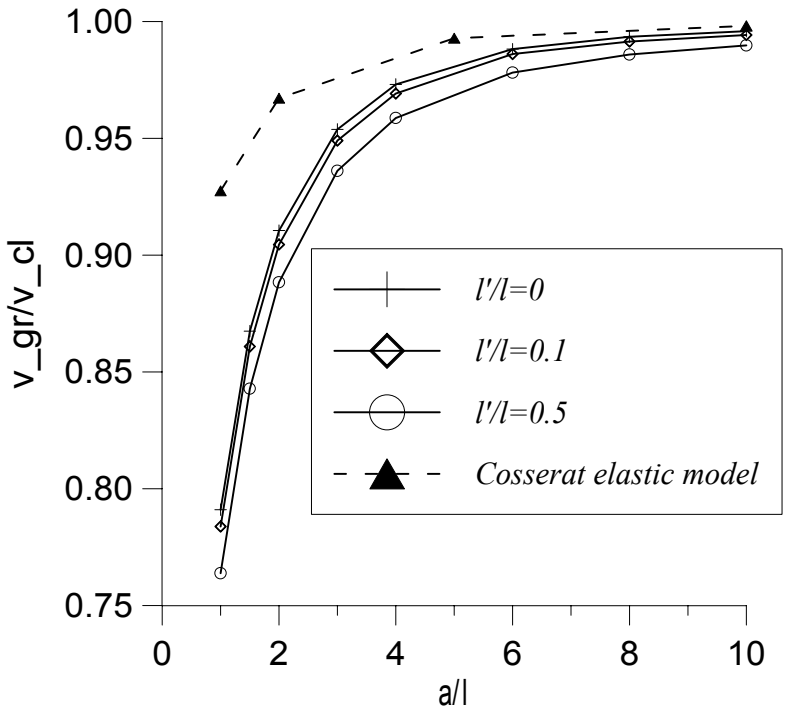

Figure 2: Scale effect for elastic 2nd-gradient and Cosserat models (Poisson's ratio = 0.3)

These results show that when the size of the indentor is comparable to the internal length of the material, for a given value of the applied pressure, the scale effect can reach 20 to 25 % in case of gradient-elasticity model and only 5 to 7% in case of a Cosserat elastic model. This

scale effect is emphasised when surface-energy terms are considered in addition to volumetric strain gradient terms.

4.2 Higher order boundary conditions

In the above section we considered the deformation of a semi-infinite elastic medium when a normal distribution of stress is applied on the boundary with zero shearing stress. If the surface is deformed by the pressure of a rigid indentor, then the appropriate boundary condition corresponds to the prescription of the normal component of the surface displacement under the indentor. However for example for the indentation of a semi-elastic medium with a rectangular indentor, the corresponding normal stress on the free surface is of the form (Johnson 1985)

$$\sigma_{yy}(x,0) = p(x) \tag{67}$$

with

$$p(x) = \begin{cases} -\dfrac{P}{\pi}\dfrac{1}{\sqrt{a^2 - x^2}} & \text{if } |x| \le a \\ 0 \quad \text{if } |x| > a \end{cases} \tag{68}$$

where P is the total force applied. This normal stress distribution is singular at the corners of the indentor ($x = \pm a$) which is in contradiction with the small strain elasticity assumption.
In addition to the classical boundary conditions considered in equations (57) and (58), the present theory allows to consider the effect of imposed double-forces at the boundary. The punching process with a rigid indentor can be represented by separating the effect of the deformation of the surface as the result of a prescribed normal stress distribution on the free surface and the effect of opening of the material at the corners of the indentor by considering appropriate higher order boundary conditions. In the following the effect of prescribing a double force at the surface of the semi-infinite elastic medium will be investigated.
Equation (54) shows that the functions $A_i(\xi)$ and $B_i(\xi)$ (i=1,2) depends only the imposed stress function at the boundary.In particular if the boundary is stress free $A_i(\xi)$ and $B_i(\xi)$ are identically zero and the remaining functions $C_i(\xi)$ (i=1,2) will be determined from the higher-order boundary conditions. Notice that in that case the stress field inside the half-plane is zero everywhere but the field of double-stresses is of course non zero.

4.2.1 The effect of a concentrated double force $\mu_{yyy}(x,0) = M\delta_0(x)$

where δ_0 is the Dirac function in 0 (Figure 3)

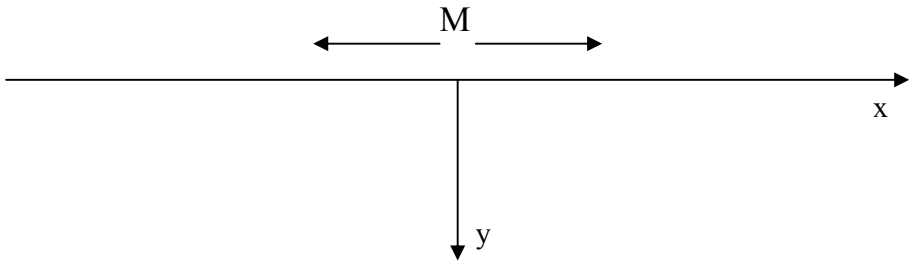

Figure 3 : Concentrated double force μ_{yyy}

for $y = 0$ and $-\infty < x < \infty$

$$\begin{cases} \sigma_{yy}(x,0) \equiv 0 \\ \sigma_{xy}(x,0) \equiv 0 \\ \mu_{yyy}(x,0) = M\delta_0(x) \Leftrightarrow \overline{\mu}_{yyy}(\xi,0) = \dfrac{1}{\sqrt{2\pi}} \displaystyle\int_{-\infty}^{+\infty} \mu_{yyy}(x,0) e^{i\xi x} dx = \sqrt{2\pi} M \\ \mu_{yyx}(x,0) \equiv 0 \end{cases} \tag{69}$$

From (55) the following expression is obtained for $C_1(\xi)$ and $C_2(\xi)$

$$C_1(\xi) = \sqrt{2\pi}\frac{M}{G} i\ell\xi \frac{\eta - \sqrt{1+\ell^2\xi^2}}{\left(m+2\left(1+\ell^2\xi^2\right)\right)\eta^2 + 2(m+2)\eta\left(\sqrt{1+\ell^2\xi^2}\right)^3 + \left(1+\ell^2\xi^2\right)\left(2(m+1)\ell^2\xi^2 + m + 2\right)}$$

$$C_2(\xi) = \sqrt{2\pi}\frac{M}{G} \frac{\eta\sqrt{1+\ell^2\xi^2} + 1 + \ell^2\xi^2}{\left(m+2\left(1+\ell^2\xi^2\right)\right)\eta^2 + 2(m+2)\eta\left(\sqrt{1+\ell^2\xi^2}\right)^3 + \left(1+\ell^2\xi^2\right)\left(2(m+1)\ell^2\xi^2 + m + 2\right)} \tag{70}$$

.

Consequently equations (52), (70) lead to the following displacement field at the boundary plane $y = 0$

$$u(x,0) = \frac{\overline{\ell}_S^2}{\ell} u^*(x,0)$$

$$u^*(x,0) = -\int_0^{+\infty} \sin\left(\frac{x}{\ell}t\right) \frac{t\left(\eta - \sqrt{1+t^2}\right)}{\left(m+2\left(1+t^2\right)\right)\eta^2 + 2(m+2)\eta\left(\sqrt{1+t^2}\right)^3 + \left(1+t^2\right)\left(2(m+1)t^2 + m + 2\right)} dt$$

$$v(x,0) = \frac{\overline{\ell}_S^2}{\ell} v^*(x,0)$$

$$v^*(x,0) = \int_0^{+\infty} \cos\left(\frac{x}{\ell}t\right) \frac{\eta\sqrt{1+t^2} + 1 + t^2}{\left(m+2\left(1+t^2\right)\right)\eta^2 + 2(m+2)\eta\left(\sqrt{1+t^2}\right)^3 + \left(1+t^2\right)\left(2(m+1)t^2 + m + 2\right)} dt \tag{71}$$

where $\overline{\ell}_S^2 = \dfrac{2M}{G}$ plays the role of a square length related to the imposed double force at the surface.

As expected it is obtained that the displacement in *x*-direction is antisymmetric whereas the displacement in *y*-direction is symmetric (Figure 4).

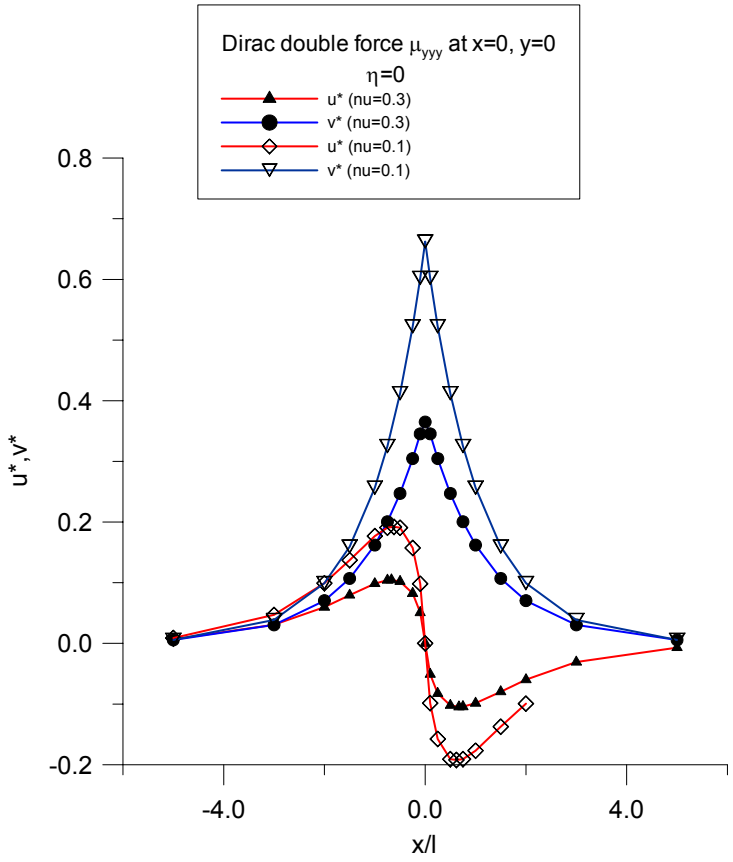

Figure 4 : Concentrated double force μ_{yyy} : displacement field

The normalised displacement increases when the Poisson's ratio ν decreases as shown on the above figure. These plots correspond to $\eta = 0$ ($\ell' = 0$). It is obtained that the maximum normalised displacement v* in y-direction obtained at the origin decreases with increasing values of the parameter η. Negative values for η correspond to a weakening of the free surface (Figure 5).

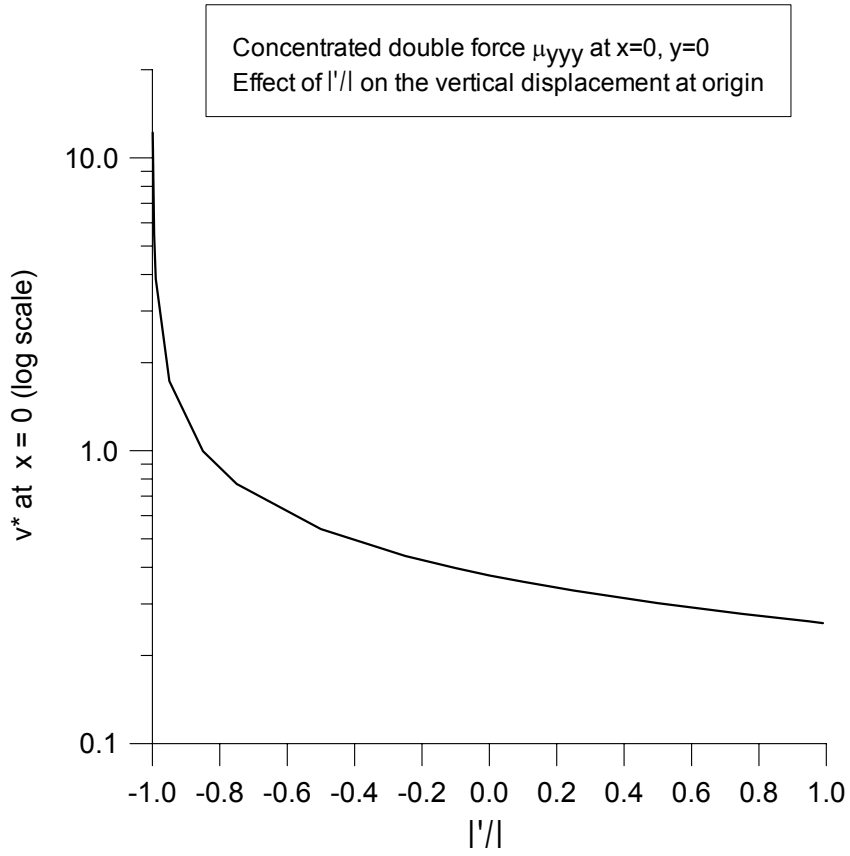

Figure 5 : Concentrated double force μ_{yyy} : The effect of the surface energy term

The effect of a double-force doublet M at x=-a and -M at x=+a can easily be obtained by superposition of the above solutions.

$$u(x,0) = \frac{\overline{\ell}_S^2}{\ell} u^*(x,0)$$

$$u^*(x,0) = 2\int_0^{+\infty} \cos\left(\frac{x}{\ell}t\right) \sin\left(\frac{a}{\ell}t\right) \frac{t\left(\eta - \sqrt{1+t^2}\right)}{\left(m+2\left(1+t^2\right)\right)\eta^2 + 2(m+2)\eta\left(\sqrt{1+t^2}\right)^3 + \left(1+t^2\right)\left(2(m+1)t^2 + m + 2\right)} dt$$

$$v(x,0) = \frac{\overline{\ell}_S^2}{\ell} v^*(x,0)$$

$$v^*(x,0) = 2\int_0^{+\infty} \cos\left(\frac{x}{\ell}t\right) \cos\left(\frac{a}{\ell}t\right) \frac{\eta\sqrt{1+t^2} + 1 + t^2}{\left(m+2\left(1+t^2\right)\right)\eta^2 + 2(m+2)\eta\left(\sqrt{1+t^2}\right)^3 + \left(1+t^2\right)\left(2(m+1)t^2 + m + 2\right)} dt \quad (72)$$

The following numerical example corresponds to a double force doublet at $\pm\ell$ (Figure 6).

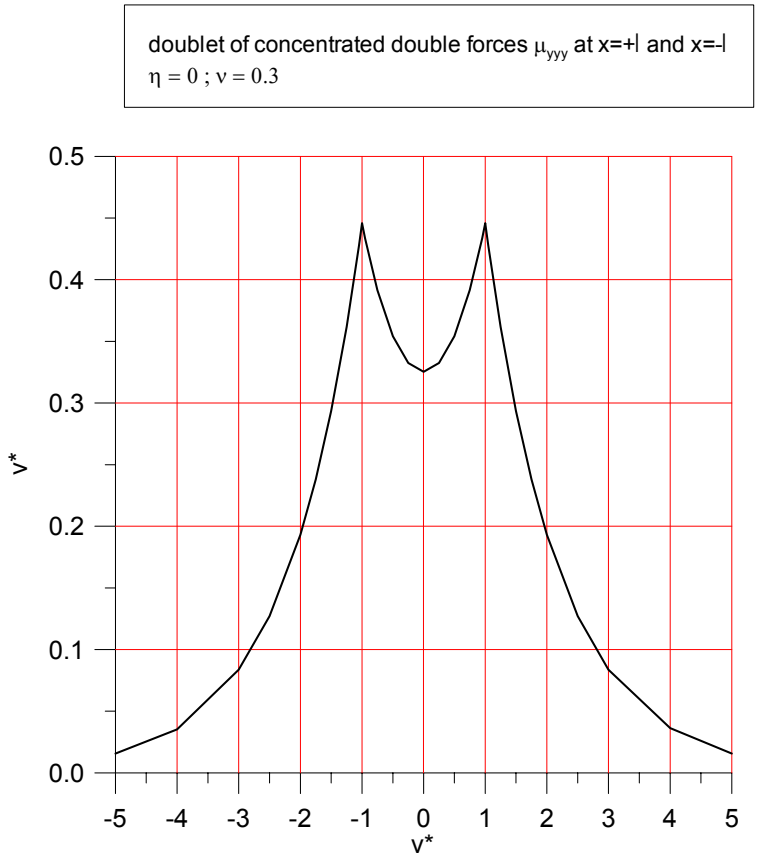

Figure 6 : Doublet of concentrated double force μ_{yyy}

4.2.2 The effect of a concentrated double force $\mu_{yyx}(x,0) = M\delta_0(x)$ (Figure 7)

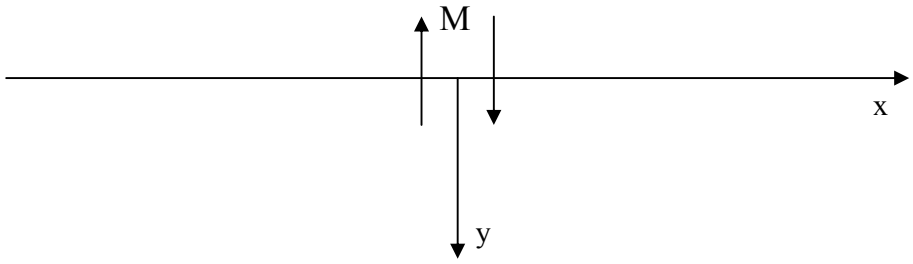

Figure 7 : Concentrated double force μ_{yyx}

The solution is derived exactly as above leading to the following expressions for the displacement field at y = 0

$$u(x,0)=\frac{\overline{\ell}_S^2}{\ell}u^*(x,0)$$

$$u^*(x,0)=\int_0^{+\infty}\cos\left(\frac{x}{\ell}t\right)\frac{(m+2)\sqrt{1+t^2}\left(\eta+\sqrt{1+t^2}\right)}{\left(m+2\left(1+t^2\right)\right)\eta^2+2(m+2)\eta\left(\sqrt{1+t^2}\right)^3+\left(1+t^2\right)\left(2(m+1)t^2+m+2\right)}dt$$

$$v(x,0)=\frac{\overline{\ell}_S^2}{\ell}v^*(x,0)$$

$$v^*(x,0)=-\int_0^{+\infty}\sin\left(\frac{x}{\ell}t\right)\frac{-mt\left(\eta+\sqrt{1+t^2}\right)}{\left(m+2\left(1+t^2\right)\right)\eta^2+2(m+2)\eta\left(\sqrt{1+t^2}\right)^3+\left(1+t^2\right)\left(2(m+1)t^2+m+2\right)}dt \tag{73}$$

This result is illustrated on the Figure 8 for the particular values $\eta = 0$ and $\nu = 0.3$.

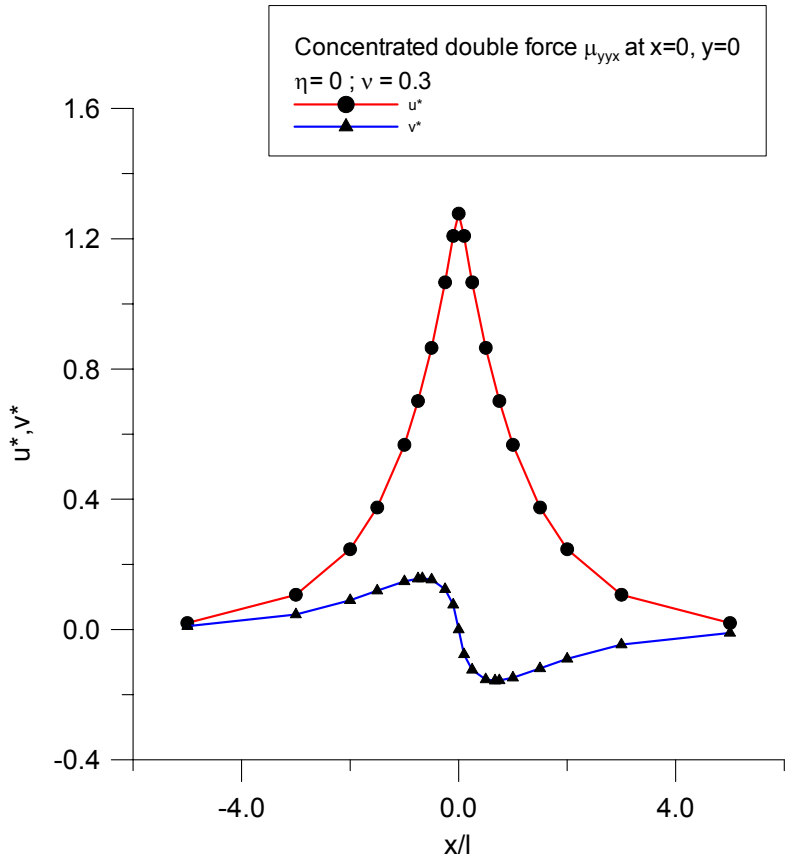

Figure 8 : Concentrated double force μ_{yyx} : Displacement field

The response for a double-force doublet at x=±a is constructed by superposition of the elementary solutions. An example is shown on Figure 9 for the normalised displacement in *y*-direction:

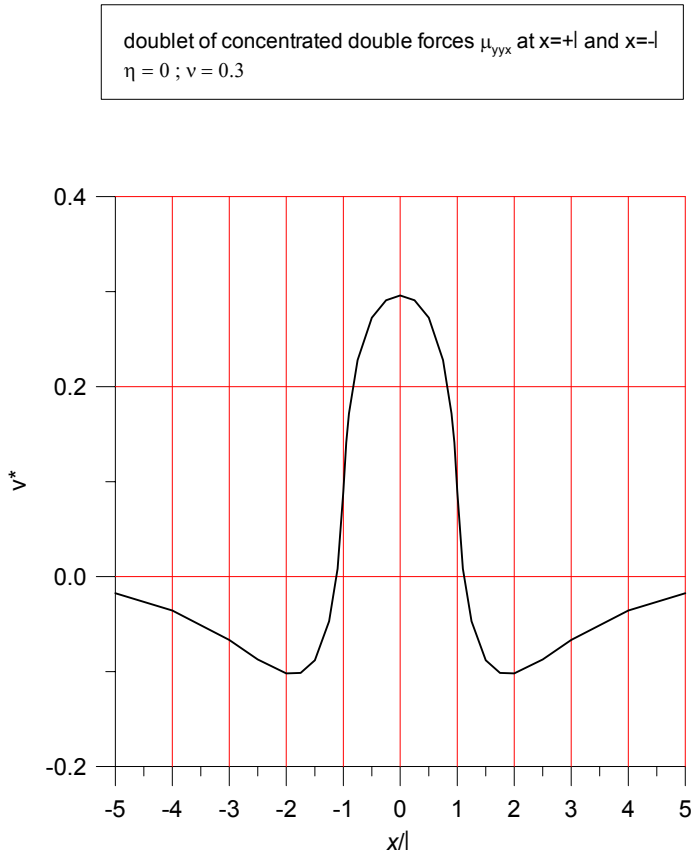

Figure 9 : Doublet of concentrated double force μ_{yyx}

4.3 Interpretation of the meaning of higher order boundary conditions

Classical boundary conditions in terms of uniform imposed pressure on the surface of the elastic half-space represents the effect of the so-called "soft" indentor. For indentation by a rigid flat punch, boundary conditions in terms of uniform imposed displacement on the surface are more appropriate. However the corresponding pressure distribution under the loaded zone calculated from classical elasticity is of the form $\frac{P}{\pi\sqrt{a^2 - x^2}}$ (Sneddon, 1951) where P is the total imposed force. The pressure reaches a theoretically infinite values at the edges of the punch ($x = \pm a$). This singularity of the stress field can be avoided by considering the indentation process as a combination of a punching process represented by a finite pressure distribution and an opening process at the edges represented by a concentrated double-force (Sulem 1999).

5 GRADIENT ELASTICITY SOLUTIONS FOR CRACK PROBLEMS IN BRITTLE GEOMATERIALS

5.1 Introduction

The first who introduced molecular forces of cohesion acting near the tip of a crack was Griffith who considered forces of cohesion as forces of surface tension being internal forces for the given body in order to develop his celebrated criterion of fracture mechanics (Griffith 1921); however, their effect on the stresses and strains was neglected by Griffith and his

theory predicts infinite slope of the crack displacement at the crack tip. Classical Linear Elastic Fracture Mechanics (LEFM) theory which was based on the concept of sharp Griffith cracks (considered as branch cuts) predicts infinite slope of the crack displacement at the crack tip. For example, for the specific case of mode-I deformation one can deduce

$$2G\frac{\partial \upsilon^c}{\partial x}(r,\pi) = -\sqrt{\frac{2}{\pi}}K_I\frac{(1-\nu)}{\sqrt{r}} \neq 2G\frac{\partial \upsilon^c}{\partial x}(r,0) = 0; \quad r \to 0 \tag{74}$$

where the superscript 'c' denotes classical LEFM solution, (r,θ) are polar coordinates fixed at the crack tip, K_I is the mode-I stress intensity factor (SIF), and υ^c denotes the crack opening displacement. As it is shown in Figure 10a the origin of the crack tip singularity lies in the fact that the originally sharp crack is widening due to the application of load into a parabolic tip (i.e. $\upsilon^c(r,\pi) \propto r^{1/2}$). From a consideration of the term $\partial\upsilon^c / \partial x$, it is evident that the infinity in the slope is directly associated with the non-zero displacement at the very tip of the rounded crack. In his milestone paper in 1921 Griffith also proceeded to the investigation of the structure of the crack tip. This investigation was performed by Griffith without any consideration of cohesive forces, hence with infinite crack slope at the tip region. Griffith made an attempt to improve this description of the crack model by considering it as an elliptical cavity with a finite radius of curvature ρ at the tip (Fig. 10a). However, according to his estimate the magnitude of ρ was of the order of intermolecular distance, which, as it was pointed out by Barenblatt (1962), clearly indicates the contradiction with the original principle on which Griffith's derivation was based, that is, the continuous distribution of matter; in a continuous medium intermolecular distances cannot in principle be considered as finite.

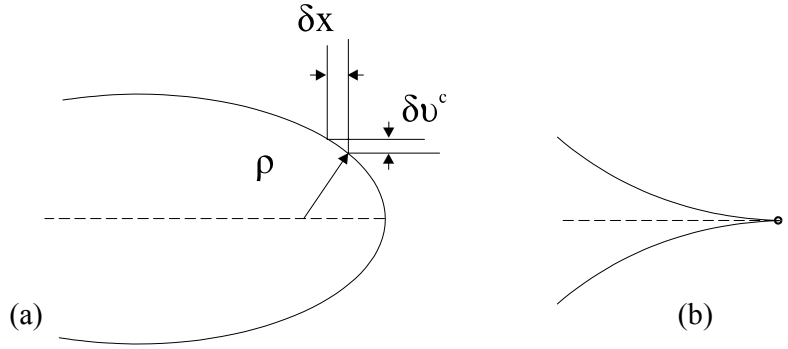

Figure 10. (a) Classical model of crack tip. Originally branch cut (broken line) opens into rounded contour (full line). (b) Crack lips in the form of a cusp of the first kind with zero enclosed angle and zero first derivative of the displacement at the crack tip ($\partial\upsilon / \partial x = 0$).

Following a different approach Elliot (1947) proposed an atomistic model which explicitly accounted for the effect of the interatomic forces along the crack faces. An important result of this study was that the adjacent atomic planes defining the crack surface displace with respect to each other *beyond the crack tip* in contrast to the results of classical elasticity. Later Barenblatt (1959) in a celebrated work has introduced a small cohesive zone ahead of the 'physical' crack tip whose size is determined *explicitly* by requiring the cancellation of stress

singularity at the tip of the cohesive zone (or tip of 'effective' crack), or equivalently smooth closure of crack lips (Fig. 10b). However, the slope of the crack opening displacement in mode-I deformation turns out to be infinite at the crack tip/cohesive zone boundary, even though a smooth closure condition is ensured. Indeed, Barenblatt (1959, p. 1013) gives the following expression for the mode-I crack opening displacement $\upsilon(x,y)$

$$\upsilon = \frac{\kappa+1}{2G}\,\mathrm{Im}(\phi(\zeta)); \quad \zeta = e^{i\theta} \tag{75}$$

with ζ-values to correspond to the contour of the crack occupying the region $-\alpha \le x \le \alpha,\ y = 0^{\pm}$, i.e. the values $\zeta = \pm 1$ correspond to the crack tips. The complex function $\phi(\zeta)$ which assures finite stresses at the crack tips is given by

$$\phi(\zeta) = \frac{\alpha}{2\pi i}\int_0^{\pi} g(\alpha\cos(\lambda))\sin(\lambda)\log\left(\frac{\zeta - e^{i\lambda}}{\zeta - e^{-i\lambda}}\right)d\lambda; \quad \lambda = \arccos\frac{x}{\ell} \tag{76}$$

and the distribution of stresses g(x) to be determined by

$$g(x) = \begin{cases} p(x) - G(x) & \alpha \le x \le \alpha + d \\ p(x) & \alpha + d \le x \le -\alpha - d \\ p(x) - G(x) & -\alpha - d \le x \le -\alpha \end{cases} \tag{77}$$

In the above expressions (77) p(x) is the intensity of the normal tensile stresses at the axis of symmetry, while G(x) is the intensity of the cohesive forces and d is the width of the 'process zone'. By substituting (77) and (76) into (75) and by performing an asymptotic analysis close to the crack tip we find

$$\begin{aligned} &2G\upsilon = (\kappa+1)B\frac{\sin\theta}{(\cos\theta - 1)^2 + \sin^2\theta}, \quad x \to \alpha^{-}; \\ &B = \frac{\alpha}{3\pi}[p_0\pi^3 - G(\alpha)\lambda_0^3 - AG(\alpha)], \quad A = \pi^3 - (\pi - \lambda_0)^3, \\ &p_0 = g(\alpha\cos\lambda), \quad \lambda_0 = \sqrt{\frac{2d}{\alpha}}. \end{aligned} \tag{78}$$

By differentiating (78) w.r.t. x one may easily obtain the result

$$2G\frac{\partial\upsilon}{\partial x} = \frac{(\kappa+1)B\alpha}{2\sqrt{2}}(\alpha - x)^{-3/2} \qquad x \to \alpha^{-} \tag{79}$$

In addition, due to (79) the asymptotical value of the dislocation density as we approach the crack tip that is given by $\eta(x) = -\partial\upsilon / \partial x$ (Lardner, 1974) turns out to be infinite. Physically this is not possible, since dislocations cannot be less than a unit Burger's vector apart.

In an effort to take into account the effect of the microstructure of the material on the solution of crack problems Sternberg and Muki (1967) have studied the Mode-I crack problem within the *linearized couple-stress theory* of elastic behavior (restricted Cosserat elasticity). The problem was reduced to a system of two Fredholm integral equations of the second kind. It was found that the shape of the crack remains elliptical, as in the classical elasticity, and stress/strain inverse square-root singularities remain, although the detailed structure of the stress/strain field is altered. Later, Eringen, Spezialle, and Kim (1977) have attacked the crack problem by using *non-local elasticity*. Their work seems to indicate that nonlocal elasticity eliminates the stress singularity at the crack tip; however, the solution seems to be approximate, in the sense that the stress boundary condition at the crack surface is not satisfied exactly.

Recently, Aifantis and co-workers (Altan and Aifantis, 1992; Aifantis, 1992; Altan and Aifantis, 1997) investigated the potential of applying gradient elasticity to crack problems which are considered as traction boundary value problems. For simplicity, Aifantis and co-workers studied only the effect of the volume energy strain gradient term ℓ whereas the concept of higher order self-equilibrating stresses doing work on higher order strain gradients was not introduced for simplicity reasons. It was found that this special theory leads to smooth closure of the crack outside the region occupied by the crack at infinity before the application of the load. The smooth closure of crack at infinity is an undesirable result of this type of formulation which may be seen in some sense as a constant load punch problem for a half-space. On the other hand, Ru and Aifantis (1993) have employed the classical boundary condition of zero displacement at the crack tip in addition to the condition of zero second order derivative of displacement along the crack faces for mode-I problem. The solution, which was given in inegral form, was limited to the crack surfaces only. Unger and Aifantis (1995) have solved the small scale yielding Mode-III crack problem by using a Riemann-Green function technique without imposing the boundary condition of the second derivative of displacement along the crack which in essence is the boundary condition for double stresses in Mindlin's theory of elasticity with microstructure (Mindlin 1964). Their solution for mode-III indicated that the leading term of the displacement near the crack tip was of higher order (i.e. $\propto r^{5/2}$) than that predicted by Vardoulakis *et al.* (1996) and Exadaktylos (1998) ($\propto r^{3/2}$). In a recent paper of Exadaktylos (1999) it has been shown that the double stress does not vanish along the segment of the crack in Unger's solution, in contrast to the solution of the boundary value problem treated in (Vardoulakis *et al.*, 1996) and this is the reason for the above observed discrepancy. New results pertaining to the proposed anisotropic gradient elasticity theory with surface energy for cracks have been also presented by Paulino *et al.* (1999). More specifically, these authors presented the application of this theory to the solution of a mode III crack in a functionally graded material by means of Fourier transform and hypersingular Fredholm integral equation techniques. As it was expected the solution indicates a cusping crack, that is consistent with Barenblatt's 'cohesive zone' theory.

The complete analytical solution of the mode-III crack problem (tearing crack) is reviewed and further developed here by using the proposed anisotropic strain-gradient elasticity theory with surface energy extending previous results by Vardoulakis and co-workers, as well as by Aifantis and co-workers, and major conclusions are presented. New results recently presented by Exadaktylos (1999) are also illustrated. The solution of the problem is derived by applying the Fourier transform technique and the theory of dual integral and Fredholm integral equations. Asymptotic analysis of the solution close to the tip gives a cusping crack with zero slope of the crack displacement at the crack tip. Cusping of the crack tips is caused by the

action of 'cohesive' double forces behind and very close to the tips, that tend to bring the two opposite crack lips in close contact. Consideration of Griffith's energy balance approach leads to the formulation of a fracture criterion that predicts a linear dependence of the specific fracture surface energy on increment of crack propagation for such crack length increments that are comparable with the characteristic size of material's microstructure. This important theoretical result agrees with experimental measurements of the fracture energy dissipation rate during fracturing of polycrystalline, polyphase materials such as rocks and ceramics. The potential of the theory to interpret the size effect, i.e. the dependence of fracture toughness of the material on the size of the crack, is also presented. Furthermore, it is shown that the effect of the volumetric strain-gradient term is to shield the applied loads leading to crack stiffening, hence the theory captures the commonly observed phenomenon of high effective fracture energies of rocks and ceramics; the effect of the surface strain-energy term is to amplify the applied loads leading to crack compliance and essentially captures the development of the 'process zone' or microcracking zone around the main crack in a brittle material. Thus, the present anisotropic gradient elasticity theory with surface energy provides an effective tool for understanding phenomenologically main crack-microdefect interaction phenomena in brittle materials.

5.2 Finite-length anti-plane shear internal crack

In this section the anti-plane shear (mode-III) crack deformation mode will be treated by employing the present anisotropic gradient elasticity theory with surface energy (section 3.1). In contrast to Griffith's approach the effect of cohesive forces on the displacements and strains is considered in this theory by including higher order gradients in the constitutive equations. For this purpose let us consider homogeneous isotropic medium uninterrupted except for the mode-III crack occupying the line segment $-\alpha< x < \alpha$, $y = 0$ with stress free faces. Let there be constant shear traction $\sigma_{yz} = \tau_\infty$ at infinity. The general solution to this problem is the superposition of the solutions to the following problems: (i) the problem of the crack-free region subjected to constant shear traction $\sigma_{yz} = \tau_\infty$ at infinity and (ii) the problem of the crack sheared out by constant shear traction $-\tau_\infty$ with no loading at infinity. Problem (i) is trivial with the following solution

$$w = \frac{\tau_\infty}{G} y, \quad \sigma_{xz} = 0, \ \sigma_{yz} = \tau_\infty, \quad \mu_{xxz} = \mu_{xyz} = \mu_{yxz} = \mu_{yyz} = 0 \tag{80}$$

Next we consider problem (ii). By symmetry reasons, the problem is equivalent to a half-plane $y \geq 0$ problem, when its boundary is subjected to the following mixed-mixed boundary conditions

$$\begin{aligned} &\sigma_{xy}(x,0^+) = -\tau_\infty \\ &\mu_{yyz}(x,0^+) = 0 \quad 0 \leq x < a \\ &w(x,0^+) = 0 \qquad a < x < \infty \end{aligned} \tag{81}$$

and to the homogeneous regularity conditions at infinity

$$\sigma_{xz}, \sigma_{yz} \to 0, \quad \mu_{xxz}, \mu_{xyz}, \mu_{yxz}, \mu_{yyz} \to 0, \quad u_z \to 0 \quad \text{as} \sqrt{x^2 + y^2} \to \infty \tag{82}$$

The first and third of (81) are the classical conditions, while the second one of conditions (81) is an extra boundary condition required as a result of the gradient terms. The first stress boundary condition in (81) is satisfied if we introduce the following *Westergaard* stress function

$$\overline{Z}_{III} = -i\tau_\infty \alpha \int_0^\infty \xi^{-1} J_1(\alpha\xi) e^{i\xi z} d\xi \tag{83}$$

The anti-plane strain or mode-III crack problem in gradient elasticity may be solved by employing the above Westergaard function and the following displacement-expression (Vardoulakis *et al.* 1996)

$$w(x, y) = w_c(x, y) + w^+(x, y) \tag{84}$$

where $w_c(x,y)$ is the harmonic real function that corresponds to the classical mode-III crack problem and $w^+(x,y)$ obeys the homogeneous Helmholtz equation, i.e.

$$\nabla^2 w_c = 0, w^+ - \ell^2 \nabla^2 w^+ = 0 \tag{85}$$

The general solution of the function $w^+(x,y)$ for the half-plane $y \geq 0$, considering the regularity conditions at infinity and the symmetry relations furnishes

$$w^+(x, y) = F_c[\{\overline{w}(\xi) e^{-ya(\xi)}; \xi \to x], y \geq 0 \tag{86}$$

wherein F_c denotes the Fourier cosine transform, $a(\xi) = \sqrt{\xi^2 + (1/\ell^2)}$. Furthermore, substituting (86) for w^+ and (83) in the expression for μ_{yyz} and considering the last two conditions (82) we are led to a system of dual integral equations for $B(\xi)$. This system may be eventually transformed into a regular integral equation of a standard form. This is accomplished by taking the following fractional integral representation for $w^+(x,0^+)$

$$w^+(x,0^+) = \sqrt{\frac{2}{\pi}} \int_0^\infty \overline{w}(\xi) \cos x\xi d\xi = \int_x^\alpha \psi(t) \sqrt{t^2 - x^2}\, dt \qquad 0 \leq x < \alpha \tag{87}$$

where $\psi(t)$ is a sectionally continuous function which may exhibit weak singularities in $[0, \alpha]$ and it is allowed to depend on ℓ, ℓ' and α. Equation (87) implies that the condition of zero displacement ahead of the crack tip is satisfied identically. Proceeding formally as it is shown in (Vardoulakis *et al.* 1996) the mixed-mixed boundary value problem problem is reduced to that of a tractable Fredholm integral equation of the second kind, that is

$$\begin{aligned} \psi(t) = &-\ell^{-2} \int_0^\alpha \tau\psi(\tau) d\tau \int_0^\infty \xi^{-1} \left[1 + \frac{\ell'}{\ell} \sqrt{1 + \ell^2 \xi^2} \right] J_1(t\xi) J_1(\tau\xi) d\xi - \\ &- \frac{\tau_\infty}{G} \left(\frac{\alpha}{t} \right)^{1/2} \delta(\alpha - t) - \frac{1}{2} \frac{\tau_\infty}{\mu} \frac{\ell'}{\ell^2} \frac{t}{\alpha}\, {}_2F_1\left(\frac{3}{2}, \frac{1}{2}; 2; \frac{t^2}{\alpha^2}\right) \quad 0 \leq t < \alpha \end{aligned} \tag{88}$$

Once $\psi(t)$ is known, the problem can be regarded as solved. The solution of the Fredholm integral equation of the second kind (88) for $(\ell'/\ell) \cong 0$ is facilitated by Liouville-Neumann method of successive substitutions provided that $\ell > 0.707\alpha$

$$\begin{aligned} &\psi(t) = -\frac{\tau_\infty}{G}(\alpha/t)^{1/2}\delta(\alpha - t) + \hat{\psi}(t), \quad \lambda = -\ell^{-2}; \\ &\hat{\psi}(t) = -\lambda\psi_1(t) + \lambda^2\psi_2(t) - \lambda^3\psi_3(t) + \lambda^4\psi_4(t) + O(\lambda^5) \end{aligned} \tag{89}$$

where throughout this paper 'O' denotes Landau's order-of-magnitude symbol, and

$$\begin{aligned} &\psi_1(t) = -\frac{\tau_\infty\alpha}{2G}\left(\frac{t}{\alpha}\right), \psi_2(t) = -\frac{\tau_\infty\alpha^3}{2G}\left[-\frac{1}{8}\left(\frac{t}{\alpha}\right)^3 + \frac{1}{4}\left(\frac{t}{\alpha}\right)\right], \\ &\psi_3(t) = -\frac{\tau_\infty\alpha^5}{2G}\left[-\frac{1}{32}\left(\frac{t}{\alpha}\right)^3 + \frac{3}{64}\left(\frac{t}{\alpha}\right) + \frac{1}{192}\left(\frac{t}{\alpha}\right)^5\right], \\ &\psi_4(t) = -\frac{\tau_\infty\alpha^7}{2G}\left[-\frac{1}{9216}\left(\frac{t}{\alpha}\right)^7 + \frac{1}{768}\left(\frac{t}{\alpha}\right)^5 - \frac{3}{512}\left(\frac{t}{\alpha}\right)^3 + \frac{19}{2304}\left(\frac{t}{\alpha}\right)\right] \end{aligned} \tag{90}$$

It can be easily shown that the zero-order approximation of the functions $-\sqrt{\alpha/t}(\tau_\infty/\mu)\delta(\alpha - t)$ *cancels out the displacement predicted by the classical elastic solution which is responsible for the infinite slope of the crack displacement at the crack tip*. Next, the Newmann expansion of the present solution for mode-III crack for zero value of the surface energy length scale, i.e. $\ell' = 0$, yields

$$\begin{aligned} &w(x,0) \cong \left(\frac{\tau_\infty}{G}\right)\frac{\ell^{-8}}{5806080}\left\{-5083\alpha^6 + 1866x^2\alpha^4 - 264x^4\alpha^2 + 16x^6 + 29376\ell^2\alpha^4\right. \\ &\left. -10368x^2\alpha^2\ell^2 + 1152x^4\ell^2 - 169344\ell^4\alpha^2 + 48384x^2\ell^4 + 967680\ell^6\right\}\left(\alpha^2 - x^2\right)^{3/2}; \\ &0 \le x < \alpha; \qquad \ell > \sqrt{2}\alpha \end{aligned} \tag{91}$$

Fig. 11 illustrates the elliptical crack shape predicted by Griffith's theory and the cusp-like shape of crack predicted by the present anisotropic gradient elasticity theory (equation 91), where both cracks display the same displacement at the centre of the crack.

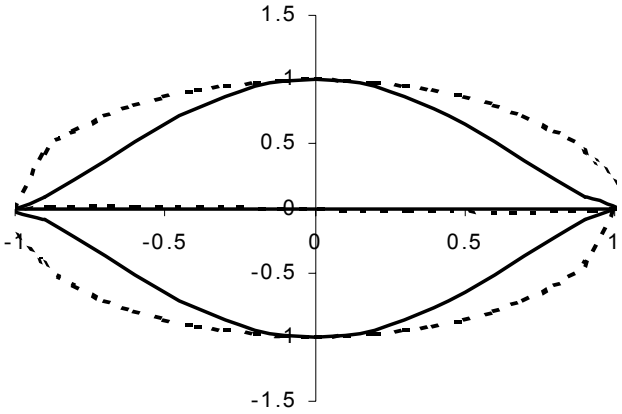

Fig. 11:Displacements on crack plane.

Further, Fig. 12 displays the crack shapes obtained from eqn (91) for $\ell / \alpha = 0.7,\ 0.8,\ 0.9$ and 1 with the crack displacements lower for higher ℓ / α - values. This crack «stiffening» effect is mainly controlled by the volumetric strain-gradient term ℓ for constant crack length (Exadaktylos, 1998).

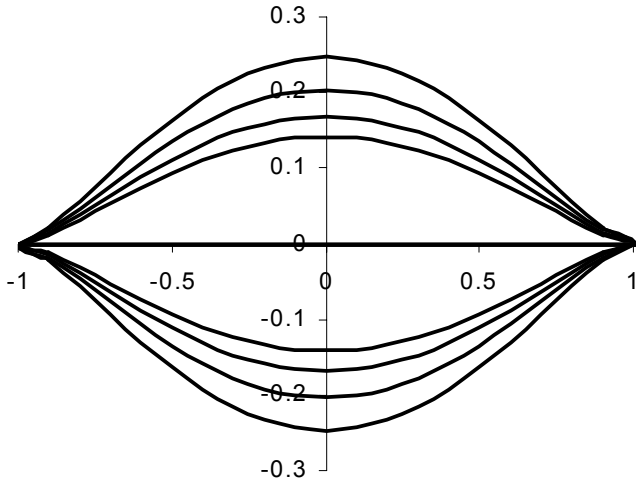

Fig. 12: Crack face displacements predicted by the present anisotropic gradient theory for four values of the relative length at hand $\ell / \alpha = 0.7,\ 0.8,\ 0.9$ and 1.

5.3 Semi-infinite anti-plane shear crack

5.3.1 Solution employing boundary condition on double stress

The following asymptotic estimate for the displacement, stress and double stress, respectively, which holds true as $r \to 0$ for every fixed positive ℓ (Vardoulakis *et al.* 1996)

$$2\mu w(r_1,\theta_1)=\frac{2}{3}\tau_\infty\sqrt{2\alpha}\,\hat{\psi}(\alpha)r_1^{3/2}\sin\frac{3\theta_1}{2},\ \sigma_{yz}=(r_1,\theta_1)=\frac{\tau_\infty\sqrt{\pi\alpha}}{(2\pi r_1)^{1/2}}\cos\frac{3\theta_1}{2},$$
$$\mu_{yyz}(r_1,\theta_1)=-\frac{\mu\ell^2}{\sqrt{2}}\hat{\psi}(\alpha)\sqrt{\frac{\alpha}{r_1}}\sin\frac{\theta_1}{2} \tag{92}$$

where the polar coordinates are indicated in Fig. 13. That is, for traction boundary value problems the proposed gradient elasticity theory predicts the same stresses as the classical elasticity solution.

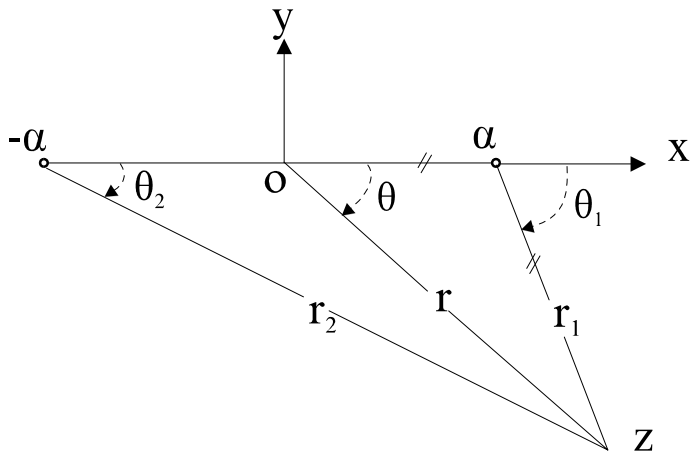

Fig. 13 Crack and coordinates.

Next, the energy released during an infinitesimal advancement of the crack tip by a distance $\delta\alpha$ is given in polar coordinates by

$$\delta U=\int_0^{\delta\alpha}\sigma_{yz}(\delta\alpha-h,0^+)w(h,\pi)\,dh \tag{93}$$

By inserting into (93) the values of w and σ_{yz} as they given by equations $(92)_1$ and $(92)_2$, respectively, and carrying out the integration we find

$$\delta U=K_{III}k_3\delta\alpha^2 \tag{94}$$

where we have set $k_3=(K_{III}/4\mu)\hat{\psi}(\alpha)$. In view of (94) and Griffith's rupture criterion (Griffith 1921)

$$\delta U\geq 2\gamma\delta\alpha \tag{95}$$

where 2γ [FL^{-1}] is the so-called 'specific fracture energy', we obtain the following inequality which involves the important physical quantity of the energy release rate G_{III} in mode-III crack propagation

$$G_{III} = \frac{\delta U}{\delta \alpha} = K_{III} k_3 \delta\alpha \geq 2\gamma \tag{96}$$

If quantity γ is independent of the crack advancement $\delta\alpha$, then the left-hand part of inequality (96) goes to zero and the gradient elasticity theory predicts that there is no contribution to the work rate from the 'holding force' on the crack extension. Since the later is not possible by fundamental physical considerations, γ has to depend linearly on $\delta\alpha$ for crack tip propagation distances that are not large as compared to the grain size of the brittle material, that is,

$$\gamma = \gamma(\delta\alpha) = \beta\delta\alpha \ \text{as} \delta\alpha \to 0 \tag{97}$$

where the quantity β has the dimensions of specific volume energy [FL^{-2}], called hereafter 'modulus of cohesion'. Then, Griffith's rupture criterion (96) is modified as follows

$$\frac{K_{III}^2}{8G} \hat{\psi}(\alpha) \geq \beta \tag{98}$$

where the left-hand-side in (98) depends on the applied pressure on the faces of the crack, on crack length and on material length parameters ℓ, ℓ'. The corresponding critical value of K_{III} which represents the fracture resistance of the material is denoted by K_{IIIC} and is called 'fracture toughness' or 'critical stress intensity factor'. Note from (98) that

$$K_{IIIC} = \sqrt{\frac{8\beta G}{\hat{\psi}(\alpha)}} \tag{99a}$$

The numerical solution of the integral equation (88) for $\ell' = 0$ and consideration of equations (89) and (99a), lead to the following expression for the normalized fracture toughness of a gradient dependent material

$$\hat{K}_{IIIC} = \frac{K_{IIIC}}{\sqrt{\beta G}} = 1 + \frac{2.3}{\alpha / \ell} \tag{99b}$$

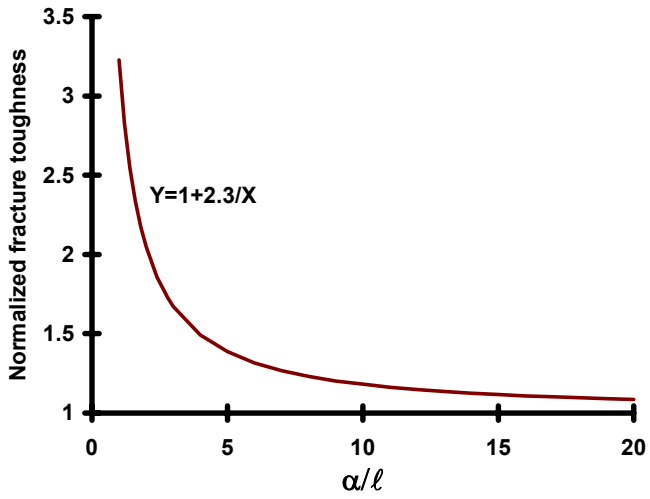

Fig. 14: Size effect of the normalized fracture toughness $\hat{K}_{IIIC} = K_{IIIC} / \sqrt{\beta G}$.

From Fig. 14 it may be seen that the resistance to fracture of the material decreases with decreasing volumetric energy parameter ℓ as it is also predicted by (99b); positive values of the surface energy parameter ℓ' further enhance the strength of the material, whereas negative values of the surface energy parameter lead to a decrease of the fracture toughness of the material (Exadaktylos 1998). Notice that LEFM does not predict an effect of the size of the crack on K_{IIIC}, that is , it considers K_{IIIC} as a constant.

5.3.2 Solution without employment of boundary condition on double stress

Here we adopt the Riemann-Green function technique adopted by Unger and Aifantis (1995). The solutions of the second of (85) in a simply-connected domain can be written as follows (Vekua 1967)

$$w^{+} = \alpha_0 I_0(r/\ell) + \mathrm{Im}\left(\int_0^z \varphi(t) I_0\left(\frac{\sqrt{\bar{z}(z-t)}}{\ell} \right) dt \right) \tag{100}$$

where $\varphi(z)$ is an analytic function, $I_n(.)$ is the modified Bessel function of the first kind and nth-order, Im(.) denotes the imaginary value of what encloses, the overbar denotes a conjugate value, and $\alpha_0 = 0$ if we take the origin of coordinates at crack tip. Integrating (100) by parts we obtain

$$w^{+} = \mathrm{Im}\left(\Phi(z) + \frac{1}{2\ell} \sqrt{\bar{z}} \int_0^z \frac{\Phi(t)}{\sqrt{z-t}} I_1\left(\frac{\sqrt{\bar{z}(z-t)}}{\ell} \right) dt \right) \tag{101}$$

Obviously solution (101) pertains to the semi-infinite crack problem since it is valid only for simply-connected regions, whereas the finite crack configuration corresponds to a multiply-

connected body. By letting $w_c = -\mathrm{Im}(\Phi(z))$ then from second of relationships (85) and (101) it is derived

$$w = \mathrm{Im}\left(\frac{1}{2\ell} \sqrt{\bar{z}} \int_0^z \frac{\Phi(t)}{\sqrt{z-t}} I_1\left(\frac{\sqrt{\bar{z}(z-t)}}{\ell} \right) dt \right) \tag{102}$$

The above methodology is more preferable than this presented above since it is amenable to general Westergaard type formulations which are known from previous elasticity solutions, for example for $r << \alpha$

$$\Phi(z) = -\frac{\bar{Z}_{III}}{G}; \bar{Z}_{III}\Big|_{z\to 0} \cong \tau_\infty \sqrt{2\alpha z} \tag{103}$$

In view of (102), (103) the out-of-plane displacement

$$w = -\frac{\tau_\infty}{2G\ell} \mathrm{Im}\left(\sqrt{\bar{z}} \int_0^z \sqrt{\frac{t}{z-t}} I_1\left(\frac{\sqrt{\bar{z}(z-t)}}{\ell} \right) dt \right) \tag{104}$$

Making the transformation of variables $t = z(1-s^2)$ the expression (104) takes the form

$$w = \frac{\tau_\infty \sqrt{2\alpha\ell}\rho}{G} \mathrm{Im}\left(\sqrt{\frac{z}{\ell}} \int_0^1 \sqrt{1-s^2} I_1(\rho s) ds \right) \tag{105}$$

where we have set the non-dimensional radius $\rho = r/\ell$ The integral appearing in (105) can be directly evaluated in closed-form (Gradshteyn and Ryzhik 1980), thus the displacement has as follows

$$w = \frac{\tau_\infty \sqrt{2\alpha\ell}}{G} \frac{\rho^{3/2}}{6} {}_1F_2\left(1; 2, \frac{5}{2}; \frac{\rho^2}{4} \right) \sin\frac{\theta}{2} \tag{106}$$

Taking into account the asymptotic expansion of the hypergeometric function for $\rho \to 0$ we find

$$w = \frac{\tau_\infty \sqrt{2\alpha\ell}}{G} \left[\frac{1}{6}\rho^{5/2} + \frac{1}{120}\rho^{9/2} + \frac{1}{5040}\rho^{13/2} \right] \sin\frac{\theta}{2} + O\left(\rho^{17/2}\right) \tag{107}$$

In view of (107) the double stress μ_{yyz} takes the following form

$$\mu_{yyz} = G\ell^2 w_{,yy} = \frac{\tau_\infty \sqrt{2\alpha}}{8} \left[(5 - 2\cos^2\theta)\sin\frac{\theta}{2} + \cos\frac{\theta}{2}\sin 2\theta \right] \sqrt{r} \tag{108}$$

which in turn gives the result

$$\mu_{yyz}(r,0)=0,\quad \mu_{yyz}(r,\pi)=\frac{3}{8}\tau_\infty\sqrt{2\alpha r} \tag{109}$$

The second of the above relations shows that the double stress does not vanish along the segment of the crack, in contrast to the solution of the boundary value problem treated in the previous paragraph. This is the reason why the former solution gives a leading term of the displacement near the crack tip that is of lower order (i.e. $\propto r^{3/2}$) than that predicted by Unger and Aifantis (1995).

5.4 The inverse mode-III crack problem

The above analysis presented in Sections 5.2 - 5.3 is based on the assumption that the traction is specified along the crack surfaces. We now consider the problem in which the crack occupies the line $|x|\le 1,\ y=0$, and the shape of the crack is prescribed, i.e. we assume that

$$w(x,0)=\varepsilon\left(1-x^2\right)^c H(1-x),\quad c\ge 1/2 \tag{110}$$

where the function $w(x)$ is uniquely prescribed for $0\le x<1$, $\varepsilon=w(0,0)$ and H is the Heaviside function. For the half-plane $y\ge 0$ it may be shown that the displacement, stresses and double stresses are given by the formulae

$$\begin{aligned}
&w(x,y)=F_c\left[A(\xi)e^{-y\xi}+B(\xi)e^{-y\sqrt{\xi^2+1/\ell^2}};\xi\to x\right],\\
&\sigma_{xz}(x,y)=-GF_s\left[\xi A(\xi)e^{-y\xi};\xi\to x\right],\ \sigma_{yz}(x,y)=-GF_c\left[\xi A(\xi)e^{-y\xi};\xi\to x\right],\\
&\mu_{yyz}(x,y)=-GF_c\left[\left(\ell'\xi-\ell^2\xi^2\right)A(\xi)e^{-y\xi}+\right.\\
&\qquad\left.\left\{\ell'\sqrt{\xi^2+1/\ell^2}-\left(1+\ell^2\xi^2\right)\right\}B(\xi)e^{-y\sqrt{\xi^2+1/\ell^2}};\xi\to x\right].
\end{aligned} \tag{111}$$

where $A(\xi)$, $B(\xi)$ are unknown real-valued functions to be determined from the boundary conditions of the problem and F_c, F_s denote the Fourier cosine and sine transforms, respectively (Gradshteyn and Ryzhik, 1980). Putting y=0 in the first of (5.38), equating the result with (110), and inverting by the Fourier cosine rule we deduce

$$A(\xi)+B(\xi)=F_c\left[\varepsilon\left(1-x^2\right)^c H(1-x);\quad x\to\xi\right] \tag{112}$$

Furthermore, satisfaction of the boundary condition

$$\frac{\partial w}{\partial y}=0\quad 0\le x<\infty,\ y=0 \tag{113}$$

yields

$$B(\xi) = -\frac{\xi}{a(\xi)} A(\xi) \quad 0 \le \xi < \infty \tag{114}$$

where $a(\xi) = \sqrt{\xi^2 + (1/\ell^2)}$. Eliminating $B(\xi)$ from (112) and (114) we get

$$A(\xi) = \frac{1}{1 - \dfrac{\xi}{a(\xi)}} F_c\left[\varepsilon\left(1 - x^2\right)^c H(1-x); x \to \xi\right] \tag{115}$$

The anti-plane shear stress along the crack-line in the transformed Fourier domain $\overline{\sigma}_{yz}(\xi,0)$ may be found from the third of equations (111) to be

$$\overline{\sigma}_{yz}(\xi,0) = -G\xi A(\xi) = -G\frac{\xi a(\xi)}{a(\xi) - \xi} F_c\left[\varepsilon\left(1 - x^2\right)^c H(1-x); \quad x \to \xi\right] \tag{116}$$

By noting the equality

$$F_c\left[\varepsilon\left(\alpha^2 - x^2\right)^c H(1-x); \quad x \to \xi\right] = \varepsilon\sqrt{\frac{2}{\pi}}\int_0^1 \left(1 - x^2\right)^c \cos x\xi d\xi = \tag{117}$$

$$\varepsilon 2^c \Gamma(1+c)\xi^{-c-1/2} J_{c+1/2}(\alpha\xi)$$

with $\Gamma(x)$ to be the Gamma function, it turns out from (116) and (117) that the stress takes the form

$$\frac{\sigma_{yz}(x,0)}{G} = -\sqrt{\frac{2}{\pi}} 2^c \Gamma(c+1)\varepsilon \int_0^\infty \frac{a(\xi)}{a(\xi) - \xi} \xi^{1/2-c} J_{c+1/2}(\xi) \cos x\xi \, d\xi \tag{118}$$

First, let us treat the «Barenblatt crack» problem corresponding to c=3/2. In this case the integrand appearing in (118) can be approximated by a linear function of ξ as it is illustrated in Fig. 15.

$$\text{ker} = \ell \frac{\ell a(\xi)}{\ell a(\xi) - \ell\xi} (\ell\xi)^{-1} \approx 2\left(\ell^2 \xi\right) \tag{119}$$

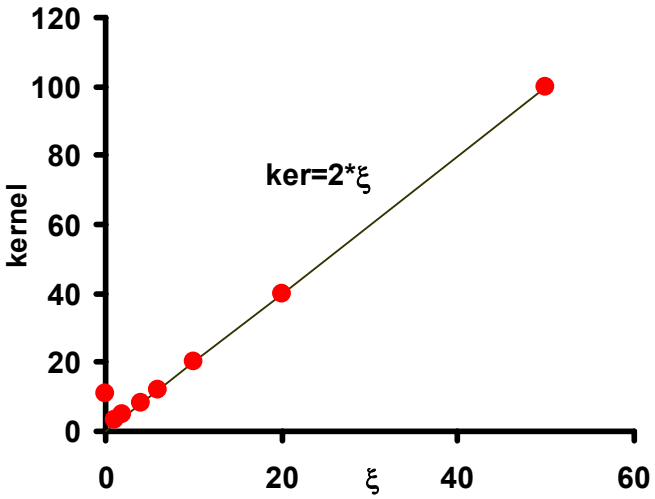

Fig. 15: Approximation of the kernel $\ker = \dfrac{a(\xi)}{a(\xi)-\xi}\xi^{-1}$ of the integrand appearing in (5.45) with a linear function

By using the above approximation the computation of the stress distribution along the crack plane can be facilitated as follows

$$\frac{\sigma_{yz}(x,0)}{12G\varepsilon} = \begin{cases} -\ell^2\, {}_2F_1\left(2,0;\dfrac{1}{2};x^2\right) & x<1 \\ -\dfrac{3\ell^2}{2x^4}\, {}_2F_1\left(2,\dfrac{5}{2};3;\dfrac{1}{x^2}\right) & x>1 \end{cases} \tag{120}$$

where ${}_2F_1(a,b;c;z)$ is Gauss's hypergeometric function.

In Fig. 15, the distribution of the normalised applied stress $-\sigma_{yz}(x,0)/12G\varepsilon$ along the crack line required for maintaining the crack cusping shape for $\ell = 1$ is illustrated. It can be demonstrated from equation (120) that as the material length scale ℓ increases the applied stress increases proportionally to ℓ^2, hence the effect of this material length is to add cohesion to the crack. Also, in Fig. 17 the distribution of the normalised tearing stress $-\sigma_{yz}(x,0)/12G\varepsilon$ along the crack line and in front of the crack tip is displayed for three values of the volumetric strain-gradient term ℓ. According to (120) this stress also increases as ℓ increases, whereas the stress singularity is larger than the inverse square root singularity exhibited in classical LEFM theory.

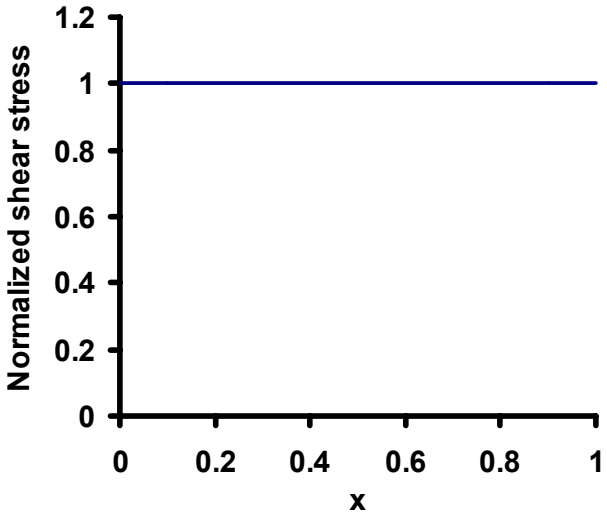

Fig. 16: Distribution of applied stress required to open the crack out to the shape shown in Fig. 12.

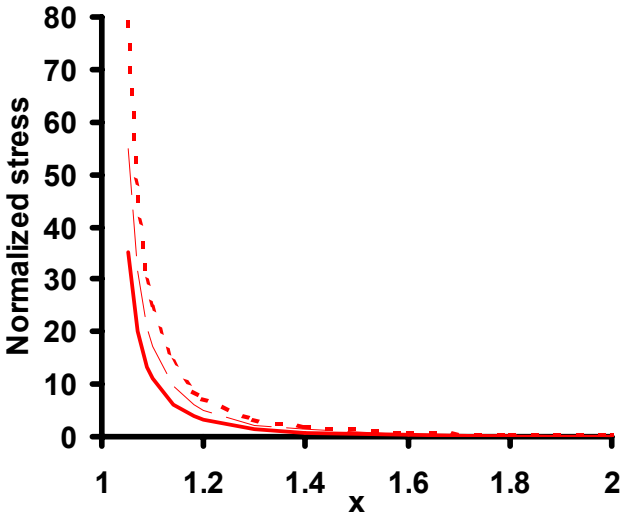

Fig. 17: Distribution of normalized tearing stress outside the crack region for three values of the volumetric strain-gradient term at hand $\ell = 0.8, 1,$ and 1.2.

5.5 Concluding remarks

Here closed form, as well as, asymptotic solutions for the mode-III crack problem were given by using a strain-gradient dependent theory of elasticity. This theory takes into account the role of the first and second gradients of strain in the mechanical behavior of elastic-perfectly brittle geomaterials, such as rocks, ceramics, and concretes. The fundamental idea behind the theory is that the effect of the granular, polycrystalline and atomic nature of materials on their macroscopic response may be modeled through the concept of internal and superficial

capillarity expressed by two material lengths ℓ, ℓ', respectively, rather than through intractable statistical mechanics concepts. The crack shape turns out to be that of a *cusp* with zero first derivative of the displacement at the crack tip. Consideration of the energy release rate in crack propagation and the Griffith criterion suggests that the specific fracture energy of a gradient elastic material is not a material property but depends linearly on the crack extension. The potential of the gradient elastic fracture mechanics theory to interpret the dependence of fracture toughness of the material on the size of the crack, is also presented. Furthermore, the solution of the inverse mode-III crack problem demonstrates that the physical meaning of the volumetric strain-gradient term is to add cohesion between crack faces hence the term «cohesive elasticity» for the present strain-gradient dependent elasticity theory.

6 CONCLUSION

The role of higher order strain gradients in the mechanical behaviour of elastic perfectly brittle materials, such as rocks, ceramics and concrete, is studied here on the basis of a special second-grade elasticity with surface energy. The fundamental idea behind the theory is that the effect of granular, polycrystalline and atomic nature of materials on their macroscopic response may be modelled through the concept of internal and superficial capillarity expressed by two material lengths, ℓ, ℓ' respectively as originally proposed by Casal (1961) and Mindlin (1964). It is shown that the important phenomenon of scale effect in rock mechanics can be interpreted by using higher order theory.

For the indentation problem, the above analysis gives an example of microstructural effects in the presence of stress concentration. For a second-gradient elasticity model, it is shown that the displacement under the indentor is 25% smaller as compared to the classical elastic solution when the size of the loading strip is comparable to the internal length of the material. This scale effect is emphasised when surface-energy terms are considered in addition to volumetric strain gradient terms. For a Cosserat elastic model the scale effect is much smaller. On the other side it was shown in a previous paper (Sulem and Cerrolaza 1999) that for a elastic perfectly plastic rock with Cosserat microstructure, the apparent strength increases as the size of the indentor decreases. This scale effect can reach 25% when the size of the indentor is comparable to the grain size of the rock. Such a scale effect has been observed experimentally for metals (Poole et al 1996) and also recently reported for rocks (Papamichos et al). In addition, indentation tests appear as an experimental tool for the testing and validation of continuum theories with microstructure and calibration of internal lengths parameters.

For crack problems, the solution of the three basic crack deformation modes with the above gradient elasticity model leads to cusping of the crack tips that is caused by the action of "cohesive" double forces behind and very close to the tips, that tends to bring the two opposite crack lips in close contact. This approach predicts a linear dependence of the specific fracture surface energy on increment of crack propagation for such crack length increments that are comparable with the characteristic size of material's microstructure. Further, it is shown that the fracture toughness depends on the size of the crack and thus is not a fundamental property of the material. Furthermore, the solution of the inverse mode-III crack problem demonstrates that the physical meaning of the volumetric strain-gradient term is to add cohesion between crack faces hence the term «cohesive elasticity» for the present strain-gradient dependent elasticity theory.

REFERENCES

Altan, B. and Aifantis, E.C. (1992). On the structure of the mode III crack-tip in gradient elasticity. *Scripta Met.* **26**, 319.

Altan, B. and Aifantis, E.C. (1997). On some aspects in the special theory of gradient elasticity. *J. Mech. Beh. Mater*. Vol. **8**, No. 3, pp. 231-282.

Aifantis, E.C. (1992). On the role of gradients in the localization of deformation and fracture. *Int. J. Engng. Sci.* **30**, 1279.

Barenblatt, G.I.(1959). Equilibrium cracks formed during brittle fracture - Rectilinear cracks in plane plates. *J. Appl. Math. and Mech*., **23**, 1009-1029.

Barenblatt, G.I. (1962). Mathematical theory of equilibrium cracks in brittle fracture. *Adv. Appl. Mech.* **7**, 55.

Casal P. (1961). La capillarité interne. *Cahier du Groupe Français d'Etudes de Rhéologie C.N.R.S.* **VI**(3), 31-37

Elliot, H.A. (1947). An analysis of the conditions for rupture due to Griffith cracks. *Proc. Phys. Soc*. **59**, 208-223.

Eringen, A.C., Speziale, C.G., and Kim, B.S. (1977). Crack-tip problem in non-local elasticity. *J. Mech. Phys. Solids*, **25**, 339-355.

Exadaktylos, G.E. (1998) Gradient elasticity with surface energy: Mode-I crack problem. *Int. J. Solids Structures* **35** (5-6), pp. 421-456.

Exadaktylos, G.E. (1999). Gradient elasticity solutions for crack problems in brittle geomaterials. In: *Proc. Int. Conf. Fracture and Damage Mechanics, July 27-29 London,* M.H. Aliabadi ed., in print.

Gradshteyn, I.S. and I.M. Ryzhik (1980). *Tables of Integrals, Series, and Products, Corrected and Enlarged Edition.* Allan Jeffrey Ed., Academic Press.

Griffith, A.A. (1921). The phenomena of rupture and flow in solids. *Phil. Trans. Roy. Soc. London* **A221**, 163, 1921.

Johnson, K.L. (1985) *Contact Mechanics*. Cambridge University Press.

Lardner, R.W. (1974). *Mathematical theory of dislocations and fracture*. University of Toronto Press, Toronto.

Kröner, E. (ed.) (1967). *Mechanics of generalised continua.* Proc. IUTAM Symposium, Freudenstadt and Stuttgart. Spinger-Verlag, Berlin.

Mindlin R.D (1963). The influence of couple stresses on stress concentrations. *Experimental Mech.* **3**, 1-7.

Mindlin R.D. (1964). Microstructure in linear elasticity. *Arch. Rat. Mech. Anal.*, **4**, 50-78.

Papamichos, E., Vardoulakis, I. and Skjaerstein, A. (1999). On the evaluation of indentation tests on reservoir rocks. In preparation

Paulino, G.H., Fannjiang, A.C., and Chan, Y.-S. (1999). Gradient elasticity theory for a mode-III crack in a functionally graded material. Materials Science Forum Vols. 308-311, pp. 971-976.

Poole, W.J., M.F. Ashby & N.A. Fleck (1996). Micro-hardness of annealed and work-hardened copper polycrystals. *Scripta Materialia,* **35**, 4, 559-564, Elsevier Science Ldt.

Ru, C.Q. and Aifantis, E.C. (1993). A simple approach to solve boundary-value problems in gradient elasticity. *Acta Mech*. **101**, 59.

Sneddon, I.N. (1951). *Fourier transforms*. McGraw-Hill, New York.

Sternberg, E. and Muki, R. (1967). The effect of couple-stresses on the stress concentration around a crack. *Int J. Solids Structures,* **3**, 69-95.

Sulem J. (1999). The role of higher order boundary conditions for rigid punching on an elastic half-space, (in preparation).

Sulem J. and Vardoulakis I. (1998) Microstructure and scale effect in rock hardness tests, in: *The Geotechnics of Hard Soils-Soft Rocks*, (ed. Evangelista & Picarelli), Vol. 2, pp. 881-888, Balkema, Rotterdam.

Sulem J. and Cerrolaza M. (1999) . Finite element analysis of the indentation test on rocks with microstructure. *Proc. Int. Conf. Fracture and Damage Mechanics, July 27-29 London,* M.H. Aliabadi ed., in print.

Unger, D.J., Aifantis, E.C. (1995). The asymptotic solution of gradient elasticity for mode III. *Int. J. Fracture* **71**, R27-R32.

Vardoulakis I. & Sulem, J.. *Bifurcation analysis in geomechanics.* Blackie Academic & Professional, 1995.

Vardoulakis, I., Exadaktylos, G. and Aifantis, E. (1996). Gradient elasticity with surface energy: Mode-III crack problem. *Int. J. Solids Structures* Vol. **33**, No. **30**, 4531-4559.

Vardoulakis I. and Exadaktylos G. (1999) Microstructure in linerar elasticity and scale effects: a reconsideration of basic rock mechanics and rock fracture mechanics, *Tectonophysics*, in print.

Vekua, I. N. (1967) *New methods for solving elliptic equations*, North Holland, Amsterdam,